NOLTR 65-43

RECALIBRATION OF THE STANDARD CARD-GAP TEST

20 AUGUST 1965

NOL

UNITED STATES NAVAL ORDNANCE LABORATORY, WHITE OAK, MARYLAND

NOLTR 65-43

NOTICE

Requests for additional copies by Agencies of the Department of Defense, their contractors, and other Government agencies should be directed to:

Defense Documentation Center (DDC)
Cameron Station
Alexandria, Virginia

Department of Defense contractors who have established DDC services or have their 'need-to-know' certified by the cognizant military agency of their project or contract should also request copies from DDC.

All other persons and organizations should apply to:

U.S. Department of Commerce
Clearinghouse for Federal Scientific and Technical Information
Sills Building
5285 Port Royal Road
Springfield, Virginia 22151

RECALIBRATION OF THE STANDARD CARD-GAP TEST

T. P. Liddiard, Jr. and Donna Price

ABSTRACT: A new calibration of peak pressure (P) vs gap length (X) is presented for the NOL standardized and modified gap tests. It is shown that experimental values of both shock velocity (U) and particle velocity (u) are required to obtain a valid P-X curve at low pressures, because the normally linear U-u curve for the gap material exhibits a discontinuity at about X = 50 mm. The initial free-surface velocity ($u_{fs} \cong 2u$) is determined by monitoring films placed at the end of the gap.

PUBLISHED OCTOBER 1965

EXPLOSION DYNAMICS DIVISION
EXPLOSIONS RESEARCH DEPARTMENT
PHYSICAL CHEMISTRY DIVISION
CHEMISTRY RESEARCH DEPARTMENT
U. S. NAVAL ORDNANCE LABORATORY
WHITE OAK, MARYLAND

NOLTR 65-43 20 August 1965

RECALIBRATION OF THE STANDARD CARD-GAP TEST

The work described in this report was carried out under Task Numbers RMMP-22149/212/F009-06-11 (Propellant and Ingredient Sensitivity) and RMMO-51042/212-1/F009-08-02 (Guided Missile Warhead Explosive Applications).

The work described in this report is the result of recent calibration (pressure vs gap length) tests, using improved techniques and methods of analysis. The information contained herein is of considerable importance to the study of explosive and propellant sensitivity.

The identification of commercial materials implies no criticism or endorsement by the U. S. Naval Ordnance Laboratory.

J. A. DARE
Captain, USN
Commander

C. J. ARONSON
By direction

Albert Lightbody
A. LIGHTBODY
By direction

TABLE OF CONTENTS

TABLES

ILLUSTRATIONS

TABLE OF CONTENTS (Con't)

INTRODUCTION

For many years gap tests have been used to characterize explosive sensitivity to shock. Although there are many variations of this type of test, basically they all have the following: (1) a donor charge; (2) a barrier (gap) of almost any material, e.g., air, plastic, or metal; (3) an acceptor charge; and (4) a means to detect reaction of the acceptor charge, usually a witness plate of metal. The gap thickness is varied until the acceptor is initiated to detonation in 50% of the trials; this critical thickness is called the 50% gap. It is, in fact, the gap length which permits transmission of the critical pressure required to initiate the acceptor to detonation.

The advantages of such a test are: (1) the experimental set-up is simple to assemble and fire; (2) the results are very reproducible; and (3) the peak pressure transmitted to the acceptor can be changed readily by altering the length of gap.

In the past one of the chief disadvantages of the test was the lack of knowledge of the pressure transmitted to the explosive acceptor. With the advent of gap calibrations, however, the significance of gap tests was greatly increased. Eyster, et al[1] * used steel witness plates against wax gaps and assumed that the same depth of dent meant the same dent-producing pressure. This was used as a measure of relative pressures although the absolute pressure was still unknown. Cachia and Whitbread[2] improved their version of a gap test by determining the peak pressure in a brass gap as a function of gap length. Similarly, Jaffe, Beauregard, and Amster[3] calibrated the gap of polymethylmethacrylate (PMMA)** used in the NOL standardized (large-scale) gap test. Because PMMA matches the impedance of explosives better than either air or metal, the stress at the end of the gap (determined by calibration) is a better approximation to the stress transmitted to the acceptor than in the case of air or metal gaps. A measurement of the critical pressure transmitted to the explosive became possible only with the determination of the non-reactive shock behavior of several high explosives[4,5,6].

The arrangement of the NOL standardized gap test is shown in Fig. 1A, and is fully described in Reference 7. The donor is a graphited tetryl pressed to a density of 1.51 ± 0.01 g/cc. The test is used to measure the 50% gap of various explosives;

* References are on page 27.
** Lucite or Plexiglas.

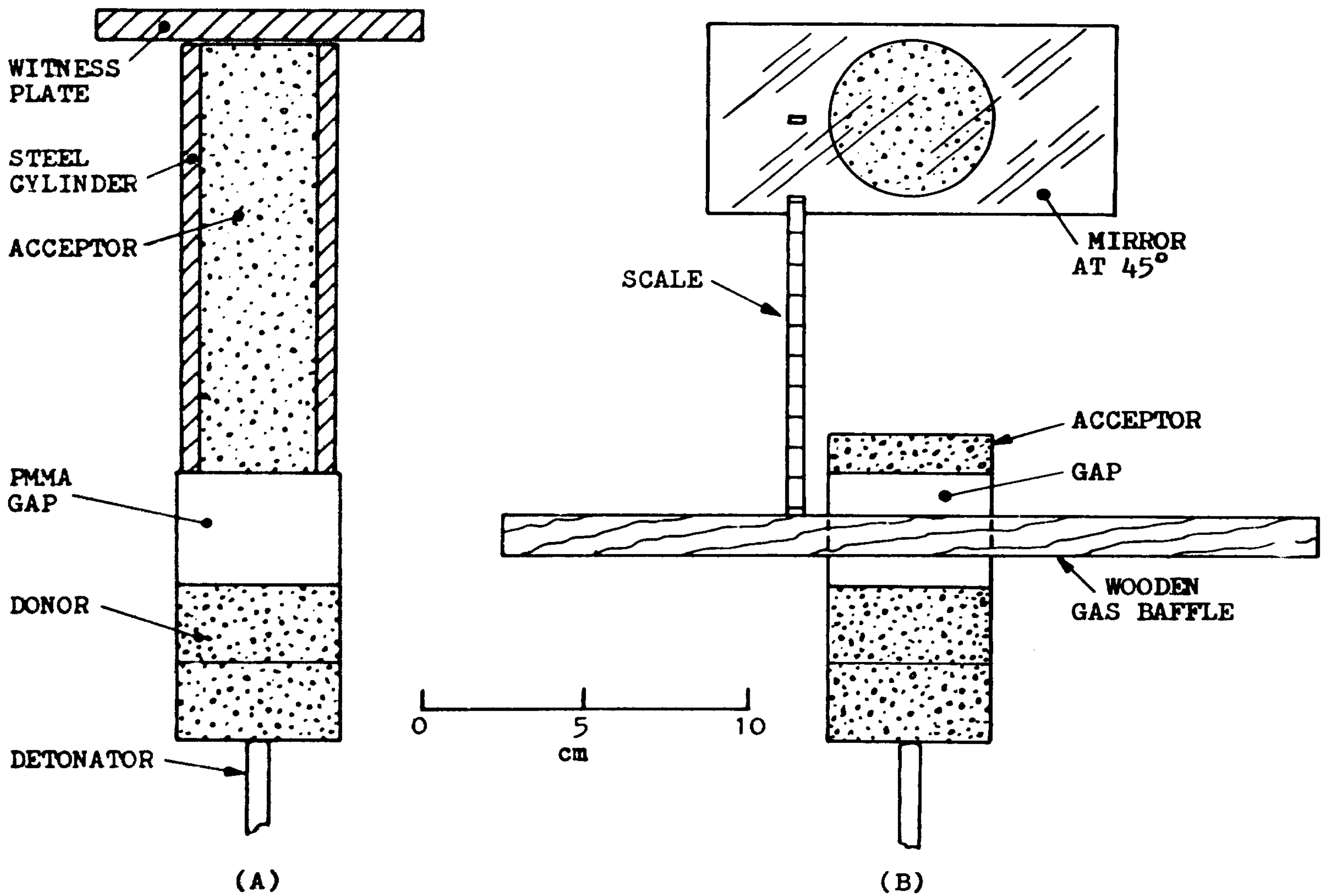

FIG. 1. (A) THE NOL STANDARDIZED GAP TEST; (B) THE MODIFIED GAP TEST.

for this purpose the criterion of a "go" is a reaction of the acceptor energetic enough to punch a hole in the steel witness plate. From the measured 50% gap and a calibration curve of peak shock pressure as a function of length of shock travel through the gap material, the shock pressure at the end of the gap is determined. This result is used with the pressure-particle velocity relation for the shocked (but unreacting) test explosive to determine the critical initiating pressure for detonation, i.e., the pressure transmitted through the 50% gap in the standardized donor/gap system.

In order to study sub-detonation reactions and at the same time to take advantage of the available calibration information, the standardized test can be modified as shown in Fig. 1B and described in Reference 8. Although the modified gap test retains the standardized donor/gap system, its acceptor is now unconfined and much shorter. Chemical reaction is detected by end-on and side-view, framing-camera surveillance of the acceptor. Burning is evidenced by the break-out of gaseous products. The curve for time of break-out (time of shock arrival at free surface to time gas is observed), determined as a function of the entering shock pressure, can be extrapolated to give the critical pressures required just to initiate the burning.

It is possible to have internal burning such that gaseous products are not visible; however, any internal burning would increase the surface velocity above that observed for a comparably shocked inert material. Consequently the free-surface velocity was also measured as a function of the entering shock pressure. Typically, the surface velocity-pressure curve shows an abrupt change in slope at the critical pressure for burning.

It is obviously important to obtain a good calibration of the donor/gap system to interpret adequately the results of both the standardized and the modified gap tests. Unfortunately, recent calibrations are not in agreement with the first one made and reported[3]. The usual calibration procedures have been found misleading; in the very important region of 20 kbar and below, they result in computed pressures which are much too high[9]. In this last case, a reliable calibration is needed to guide the necessary revisions of earlier practices.

The purpose of the present work is, therefore, to use the improved experimental and data reduction techniques developed in the last few years to obtain a calibration with the best data now available. This report documents such a calibration; it also presents in Appendix A the data from several recent previous calibrations; the data (U vs X) are correct, but their previous treatment is now superseded by the present calibration.

CALIBRATION PROCEDURE

In the gap test the gap length is altered to change the peak pressure transmitted to the acceptor. In making a calibration, the peak pressure (P) of the shock in the gap is obtained as a function of the distance (X) the shock has traveled along the axis. To determine P, both the shock velocity (U) and the particle velocity (u) must be known. The equation relating U and u with P is

$$P = \rho_0 \, u \, U,$$

where ρ_0 is the initial density of the gap material.

In the earlier calibrations only the shock-front motion was recorded, i.e., the distance (X) the shock had traveled as a function of time (t). The observations were made with a 35-mm smear camera at a writing speed of 1.3 mm/μsec. The shock velocity at a chosen position of X was determined from slopes obtained from plots of X-t read from the smear record. The corresponding particle velocity, u, was obtained from the simple relation

$$U = a + bu \; .$$

The constants a and b were obtained from other experimental work which indicated that the linear relationship held down to a pressure of about 4 kbar.[3,10,11] U vs X data obtained from recent gap calibrations, and the procedures for the reduction of shock-velocity data to gap pressures are given in Appendix A. The U-X data given there for the standardized donor/gap system provides half the data for the final P vs X curve; the remainder were obtained with the 70-mm camera, as described below.

As part of the latest calibration u, as well as U, was experimentally obtained as a function of X. Actually, the free-surface velocity of the gap (u_{fs}) was measured, u being obtained from the well-known approximation, $u_{fs} = 2u$.[12] The measurement of u is the more significant contribution to the latest calibration since the measurement of <u>both</u> u and U greatly increases the reliability of the calibration in the low-pressure domain. In addition, the U vs X curve had already been reasonably well determined, as a comparison between this latest data and that of Appendix A will subsequently show.

Measurement of Shock Velocity

A typical experimental setup for obtaining U with a smear camera is shown in Fig. 2A and a corresponding smear record in Fig. 2B. Here the gap is modified to allow light from behind to pass through two flattened regions, 50 mm apart, on the otherwise cylindrical PMMA rod. The flats are parallel to each other and to the axis of the cylinder. The slit of the smear camera is aligned along the middle of these two opposite flats. A lens placed in front of an exploding wire light source gives roughly parallel light. Actually the light is set to converge slightly so that most of the light passes through the front lens of the smear camera. The almost parallel light minimizes unwanted reflections from the curved shock front in the gap. Such reflections lead to the recording of spurious shock-front positions.

The writing speed of the smear camera, used in these experiments, was 2.5 mm/usec. Speeds of 3.8 mm/usec or more are possible with this (70-mm) camera, but these higher speeds stretch the trace excessively (in time) in relation to the space dimension (length) covered by the slit. This results in a loss of slope-measuring accuracy.

In some shots a baffle of PMMA is inserted between the gap and the donor, as shown in Fig. 2A. The insertion adds 3.2 mm to the gap length. In other shots a wooden collar baffle, shown in Fig. 1B is used, the gap material passing through a hole in the baffle. A seal around the hole is made with putty.

The shock-velocity data obtained with the 70-mm smear camera and a discussion of how the records were analyzed are given in Appendix B. As mentioned before, recent shock-velocity data, obtained with the 35-mm camera, is in Appendix A.

Measurement of the Surface Velocity

In making measurements of u, both smear and framing cameras are used. The displacement of the free end of the gap is obtained as a function of time along the extended axis of the gap. The motion initially given to the surface of the gap is retarded quickly because of rapidly falling pressures; the rapid decay results from the arrival of rarefactions, both lateral and from behind. This presents a problem since it is the initial free-surface velocity of the gap material that must be obtained. It is useless to attempt to measure the initial slope on the smear record. An air shock moving ahead of the surface causes large errors in the apparent gap-surface position for the first 1 - 2 mm of travel. This source of error could be eliminated by removing the air. However, it is doubtful if the resolution of

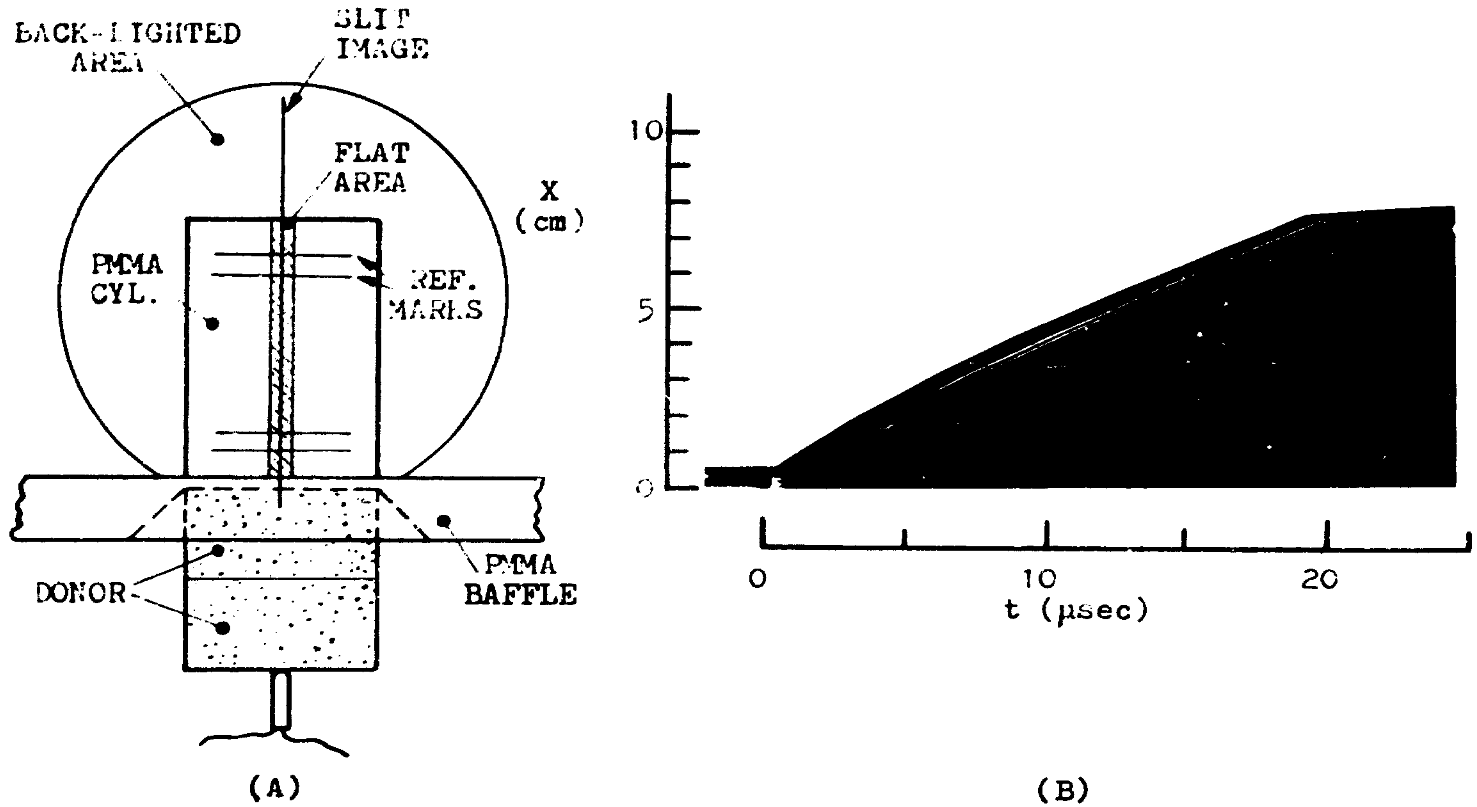

FIG. 2. (A) TEST SET-UP FOR OBTAINING THE SHOCK VELOCITY WITH A SMEAR CAMERA;
(B) TYPICAL SMEAR RECORD.

the camera, both in time and space, would give reliable measurements even in vacuo. The problem is solved by placing thin foils of the proper material and size on the gap. If the foil is thin enough and has a shock impedance higher than (or equal to) the gap material, it acquires a velocity which is nearly twice the particle velocity in the gap material. This statement is made without mathematical proof, but it is supported by experiment. In addition, the following reasoning can be used. On the first pass of the shock through a foil of higher impedance than PMMA, the free-surface velocity of the foil will be lower than the velocity the PMMA surface would have had without the foil. However, the mass of the foil is extremely low in comparison to the mass pushing it. Thus, it will be forced to adjust to the velocity of the mass from behind after several transits of shocks and rarefactions through the foil. The foil will remain in contact with the gap material until pressure immediately behind the foil begins to fall. When this happens separation occurs since there is virtually no tensile strength between the foil and the gap surface. No cement is used to attach the foil, only a trivial amount of silicone grease to hold it in place.

A typical arrangement for a smear-camera measurement of u_{fs} is shown in Fig. 3A, along with the X-t trace, Fig. 3B. A 5° bevel at the top of the gap, used in some of the tests, gives a sharp recording of the edge of the flat region on which the foil is placed. In the smear record the retarded gap surface can be seen moving behind the foil. The trace of the air shock, moving ahead of the foil, is faint and has been retouched for reproduction.

Because of the greatly restricted spatial observation obtained with the smear camera, framing camera observations were made also. The latter leave no doubt as to what is being recorded. A Jacobs camera[13,14] sequence of a 0.025-mm thick brass foil separating from a 100-mm long PMMA cylinder is shown in Fig. 4. The charge assembly is essentially the same as that used in obtaining the smear record in Fig. 3. The interval between frames is 8.16 μsec. More precisely, the interval is measured between identical horizontal positions in the field of view, since a focal plane shutter (vertical slit) is used. The frames are completed (swept) from left to right.

A number of shots were made before the foil technique was satisfactorily developed. Tables 1 and 2 contain the earlier data (retarded surface velocities). Table 3 contains the free-surface velocities measured by the foil technique after its perfection. Fig. 5 compares the curves of the retarded and the foil velocities as functions of the gap thickness.

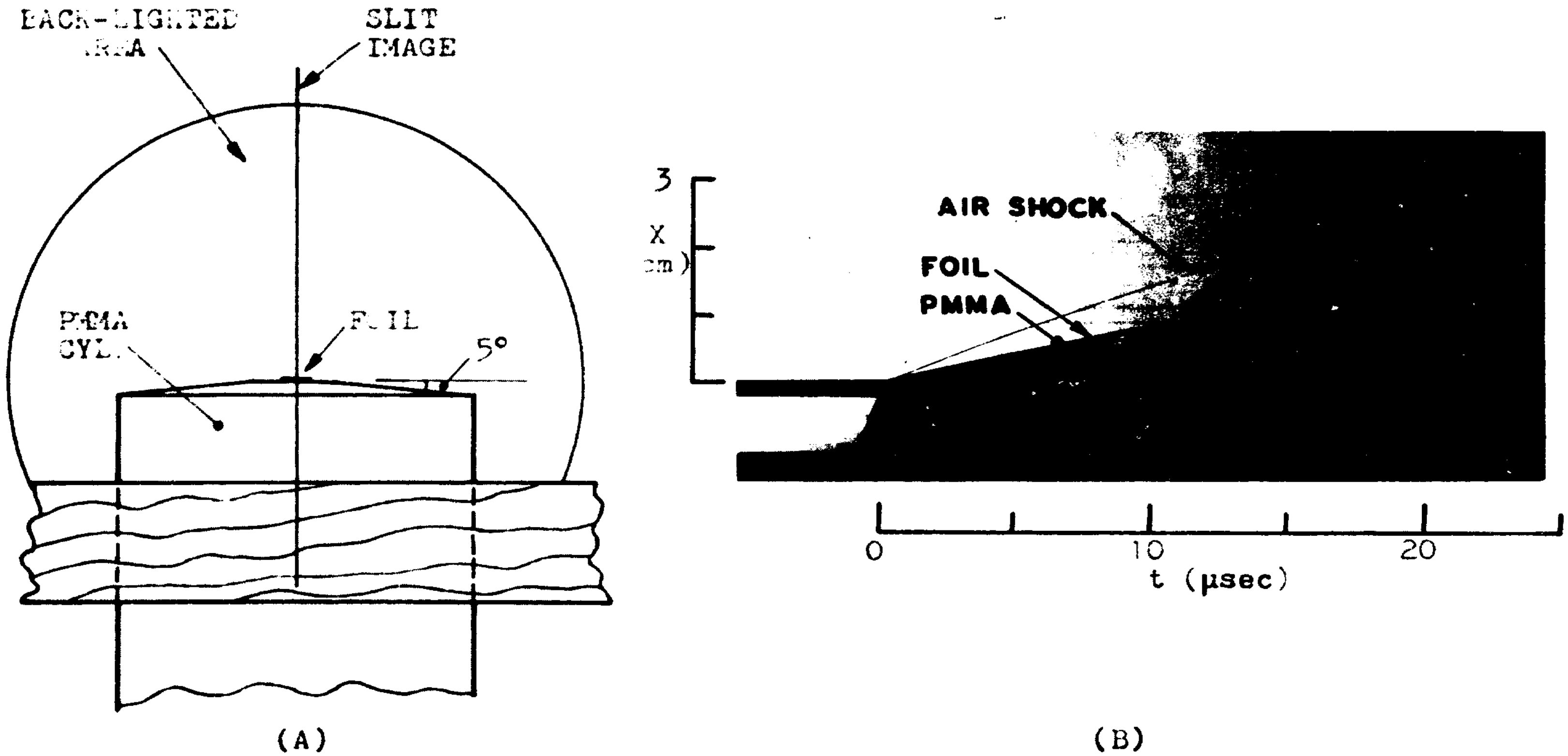

FIG. 3. (A) TYPICAL SMEAR-CAMERA SET-UP FOR MEASURING THE FREE-SURFACE VELOCITY;
(B) CORRESPONDING SMEAR RECORD.

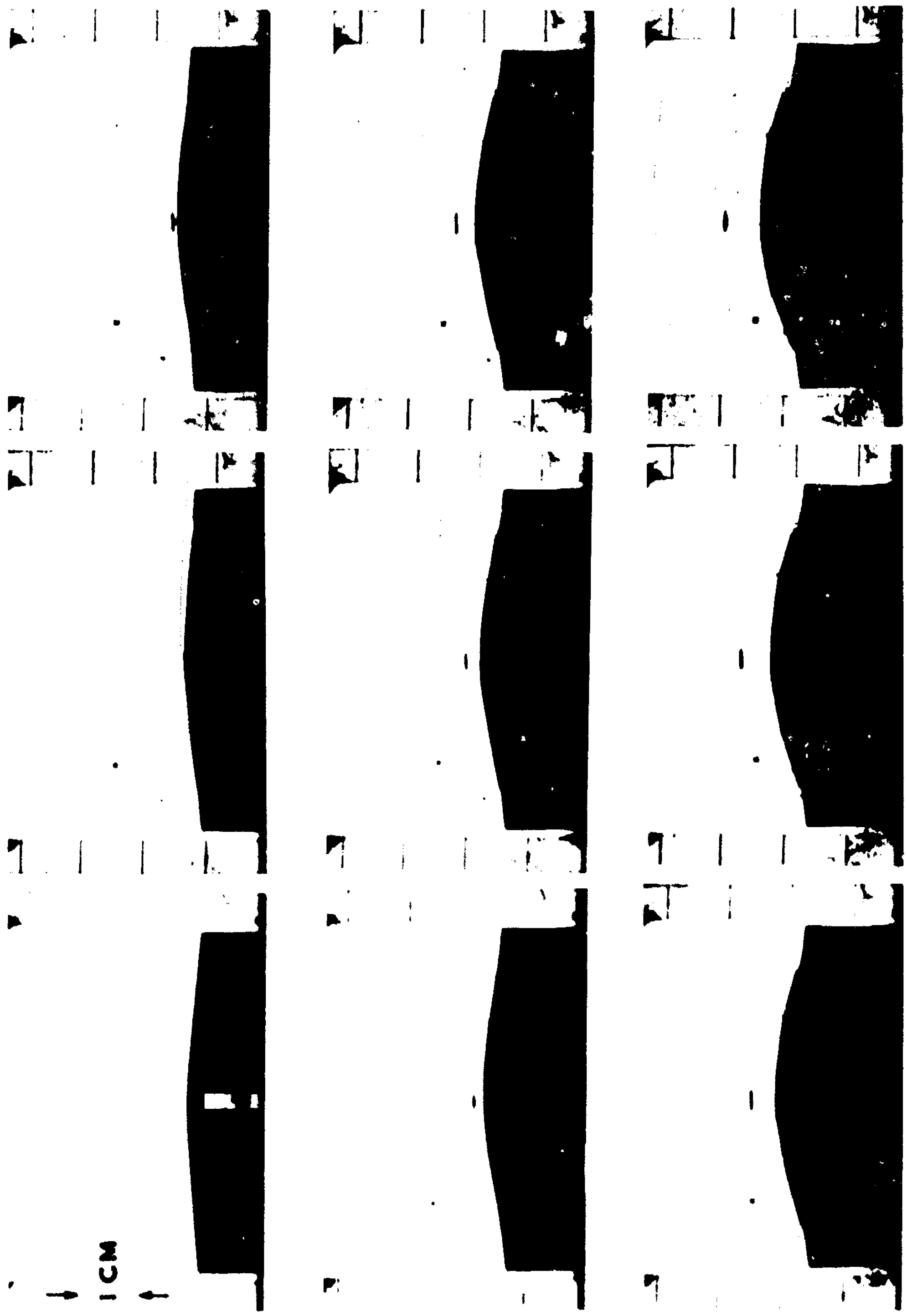

FIG. 4. FRAMING-CAMERA SEQUENCE OF A 0.025-mm THICK BRASS FOIL SEPARATING FROM THE PMMA SURFACE. (INTERFRAME TIME: 8.2 μsec)

TABLE 1

RETARDED FREE-SURFACE VELOCITY MEASUREMENTS OF PMMA GAPS

Shot	Length of Gap[a] (mm)	u_{fs} (retarded) (mm/μsec)
	No foil on PMMA surface	
144 D	47.6	0.927
C	55.2	0.699
B	65.5	0.480
A	86.0	0.264
	Surface covered by foil[b]	
144 N	10.0	2.742
M	20.0	2.110
F	29.4	1.736
E	36.0	1.411
L	43.0	1.115
K	75.0	0.377
J	99.9	0.211

[a] Includes 3.2 mm PMMA baffle.

[b] Mylar film 0.05-mm thick, 49-mm diam; no detectable separation of film from surface.

TABLE 2

EQUIVALENCE OF DONOR SYSTEMS IN FREE-SURFACE VELOCITY MEASUREMENTS

Shots	Length of Gap[a] (mm)	u_{fs} (retarded) (mm/μsec) Donor System[b] (1)	(2)
144 A, H	86.0	0.264	0.278
C, I	55.2	0.699	0.688
E, G	36.0[c]	1.411	1.419

[a] Includes 3.2 mm PMMA baffle.

[b] System (1): Tetryl from lot CH 5213 and Hercules J-2 special blasting cap. Donor system used in the modified gap test.

System (2): Tetryl from lot 1878-96 and No. 6 Olin Mathieson blasting cap. Donor system used in standardized gap test.

[c] Mylar film, 0.05 mm thick, 49-mm diam, on PMMA free surface; no detectable separation from gap surface. Film used only for shots E and G.

TABLE 3

FREE-SURFACE VELOCITY MEASUREMENTS USING SMALL-DIAMETER FOILS

Shot No.	Length of Gap[a] (mm)	Foil			u_{fs} (mm/usec)	
		Material	Thickness (mm)	Diam (mm)	PMMA (retarded)	Foil (true)
144 O	100.1	Mylar	0.05	14	0.206	0.278
P[b]	100.1	Mylar	0.05	14	0.207	0.291
Q[b]	100.1	Mylar	0.05	3-4	0.205	0.263
R[b]	100.1	Mylar	0.05	3-4	0.210	0.296
S[b]	100.0[c]	Saran	0.006	3	0.213	0.292
147[d]	100.0	Mylar	0.05	3-4	0.208	0.290
157[d]	100.0	Al	0.025	4	0.189	0.266
158[d]	100.0[c]	Brass	0.025	4	0.199	0.276
159[d]	20.0	Mylar	0.05	3-4	2.086	2.174
149[d]	45.0	Mylar	0.05	3-4	1.009	1.078
144 T[b]	75.0	Saran	0.006	3	0.375	0.427
144 U[b]	152.5	Saran	0.006	3	-	0.155

a Includes 3.2 mm PMMA baffle except for shots P through U.

b Plywood baffle in place of PMMA baffle. It is a sealed collar 18-mm thick and is placed 12-13 mm from end of gap. See Fig. 1B.

c Gap beveled (5° with flat end) with 3.5- to 6.5-mm diameter platform.

d Jacobs camera used; all others with smear camera.

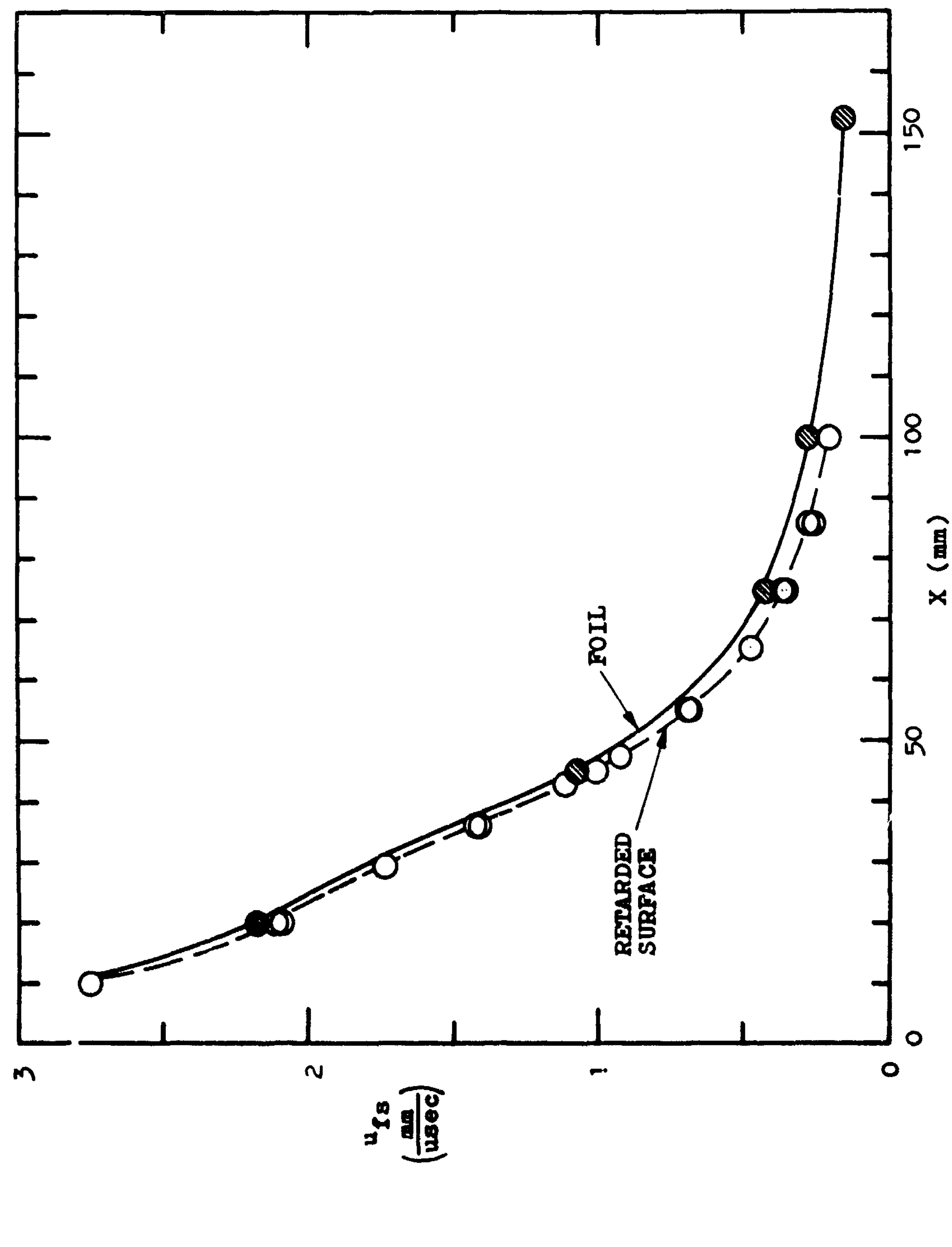

FIG. 5. RETARDED SURFACE VELOCITY AND FOIL VELOCITY AS FUNCTIONS OF PMMA THICKNESS.

The difference between the foil and retarded surface velocities is 0.05 to 0.09 mm/μsec. The threshold velocity in spall reported[15] for PMMA is 0.06 mm/μsec. It is therefore reasonable to attribute the observed amount of retardation to the structural tensions of the material which act to delay spall formation.

The data of Table 1 (included in retarded surface curve, Fig. 5) show that 49-mm diameter foils failed to separate from the free surface of the PMMA and exhibited the same retarded velocity observed for the surface without a foil. The data of Table 3, however, show that foils of diameters of 14 mm and less did separate from the surface and exhibited higher velocities*; the lack of effect of diameter at and below 14 mm indicates that the maximum possible separation between the PMMA surface and the foil had occurred at 14 mm. The data of Table 3 also show that changing the foil material or thickness, within limits, does not alter foil velocity significantly. For a 100-mm long gap, foils of Mylar, Saran, aluminum, and brass all exhibit velocities within the range of 0.26 to 0.30 mm/usec. At the same gap pressure, the thinner (0.006 mm) plastic foil travels no faster than does the thicker (0.05 mm) foil.

Two other experimental variations were made during the development work. One showed that tetryl Nb 1878-96 initiated by a No. 6 Olin-Mathieson blasting cap (used in standardized gap test work) and tetryl CH 5213 initiated by a Hercules J-2 special blasting cap, U. S. Army Spec 49-20 (used in the modified gap test) give equivalent results; see Table 2. So, too, do the PMMA and plywood gas baffles; see Table 3.

DERIVATION AND DISCUSSION OF CALIBRATION CURVES

Table 4 contains the **smoothed** u-X and U-X data obtained with the 70 mm camera as well as the derived values for P. All u-X data, obtained from foil velocities, are displayed in Fig. 5; the U-X data in Fig. 6. The latter illustration shows the range of U values measured at each point. Data for the ranges appear in Table B2 of Appendix B. The maximum spread amounted to ± 0.10 mm/usec, and occurred at both X = 5 and X = 35 mm.

Fig. 6 is of particular interest because it shows, in addition to the usual exponential decay of shock amplitude with distance of travel through a condensed medium, an increased degree of attenuation starting at X = 25 mm. As a result, for the range in X of 25 to 40 mm, there is a broad, low hump in the U-X curve. To be sure, the amount of this departure from a more regular decay curve is never greater than the experimental

* Foils having diameters between 14 and 49 mm were not tested.

TABLE 4

SMOOTHED VALUES OF PARTICLE VELOCITY (u), SHOCK VELOCITY (U), AND PRESSURE (P) AT VARIOUS DISTANCES IN THE PMMA GAP (X)

1	2	3	4	5	6
X (mm)	u (mm/μsec)	U (mm/μsec)	P (kb)	P_u[a] (kb)	P_U[b] (kb)
5	-	5.30	-	-	101
10	1.420	4.95	82.9	84	83
15	1.210	4.62	66.0	6[illegible]	67
20	1.088	4.40	56.5	57	56
25	0.990	4.21	49.2	50	49
30	0.890	4.06	42.6	43	42
35	0.780	3.88	35.7	36	35
40	0.650	3.66	28.1	28	27
45	0.538	3.46	22.0	22	22
50	0.455	3.35	18.0	18	19
55	0.383	3.30	14.9	15	17
60	0.325	3.24	12.4	12	16
70	0.245	3.17	9.2	8.6	14
80	0.200	3.13	7.4	6.8	12
90	0.168	(3.12)*	6.2	5.6	12
100	0.145	(3.10)*	5.3	4.8	11
130	0.100	(3.00)*	3.5	3.2	9
130	0.100	(3.10)**	3.7	3.2	11

[a] $P_u = 11.8u\ (2.56 + 1.69u)$

[b] $P_U = 11.8U\ (U - 2.56)/1.69$

* Values from Table A4

** If no change in velocity after X = 100 mm.

precision as judged from the data spread. Thus the present data cannot unambiguously establish such an irregularity. They do, however, strongly suggest it by exhibiting a similar irregularity at the same place in the u-X curve (Fig. 5). Finally, X = 25 mm is a shock travel path of one radius; it is therefore the location at which lateral rarefaction effects would first be expected and have been observed[9]. In other words, the small irregularities of Figs. 5 and 6 could be explained as dimensional effects.

Another irregularity, far more startling than the above, is the discontinuity in the U-u curve shown in Fig. 7. The curve is formed by plotting the values of U and u given in Columns 2 and 3 of Table 4. The values were obtained graphically at given intervals of X. Data for the first 45 mm of shock travel through the PMMA give

$$U = 2.56 + 1.69\ u \qquad (1)$$

where the units are mm/μsec. This linear relation is the form generally observed in shocked materials. The two constants are very close to those reported for PMMA by other workers, e.g., (2.59, 1.51)[3], (2.71, 1.57)[10], and (2.74, 1.35)[11]. However, the discontinuity at about U = 3.5, u = 0.5 mm/μsec (20 kbar) and the lower slope curve for the velocity relation thereafter has not, to our knowledge, been observed before. It is contradicted by the four U-u points[3] measured about five years ago by following the shock in water off the ends of 102-mm and 127-mm long PMMA cylinders. As shown on Fig. 7, these data, obtained from charges of the same dimensions as those used in the present work, fall near the extrapolation of Eq. (1) below 0.5 mm/μsec. The present work does not require data extrapolation as did the earlier[3]. Present results are more precise and more consistent with observed effects. Therefore we believe the earlier data to be in error, and the discontinuous solid line of Fig. 7 to give the most accurate measurements we can now make.

In Table 4 are listed $P = \rho_0 Uu$ where $\rho_0 = 1.18$. These pressure values are compared with P_u and P_U, values computed by use of Eq. (1) and the data for the single variable u or U, respectively. It is obvious that for path lengths up to X = 45 mm, all three methods give essentially the same pressure values. For X > 48.75 mm and P < 20 kbar, pressures computed from u alone (P_u) or U alone (P_U) depart increasingly from P. The divergence arises, of course, from the use of Eq. (1) in the low-velocity region where it is no longer applicable. Also, because of the nature of Eq. (1), its use in the low-velocity region with measured values of u leads to better estimates of P than with measured values of U, i.e., P_u is a better approximation to P than is P_U as comparison of the values in Table 4 demonstrates.

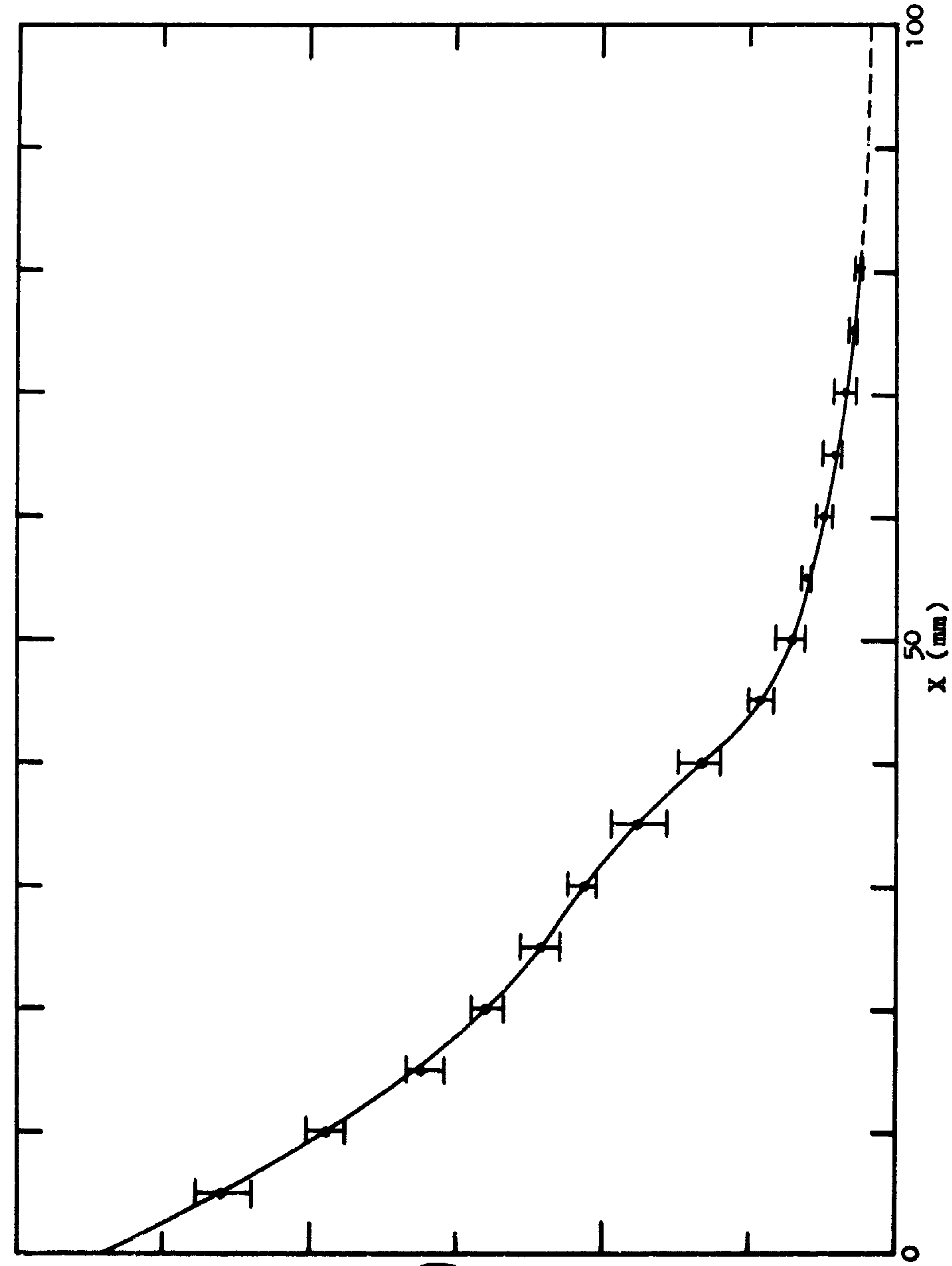

FIG. 6. SHOCK VELOCITY (U) IN THE PMMA GAP AS A FUNCTION OF THE DISTANCE (X) THE SHOCK HAS TRAVELED IN THE GAP.

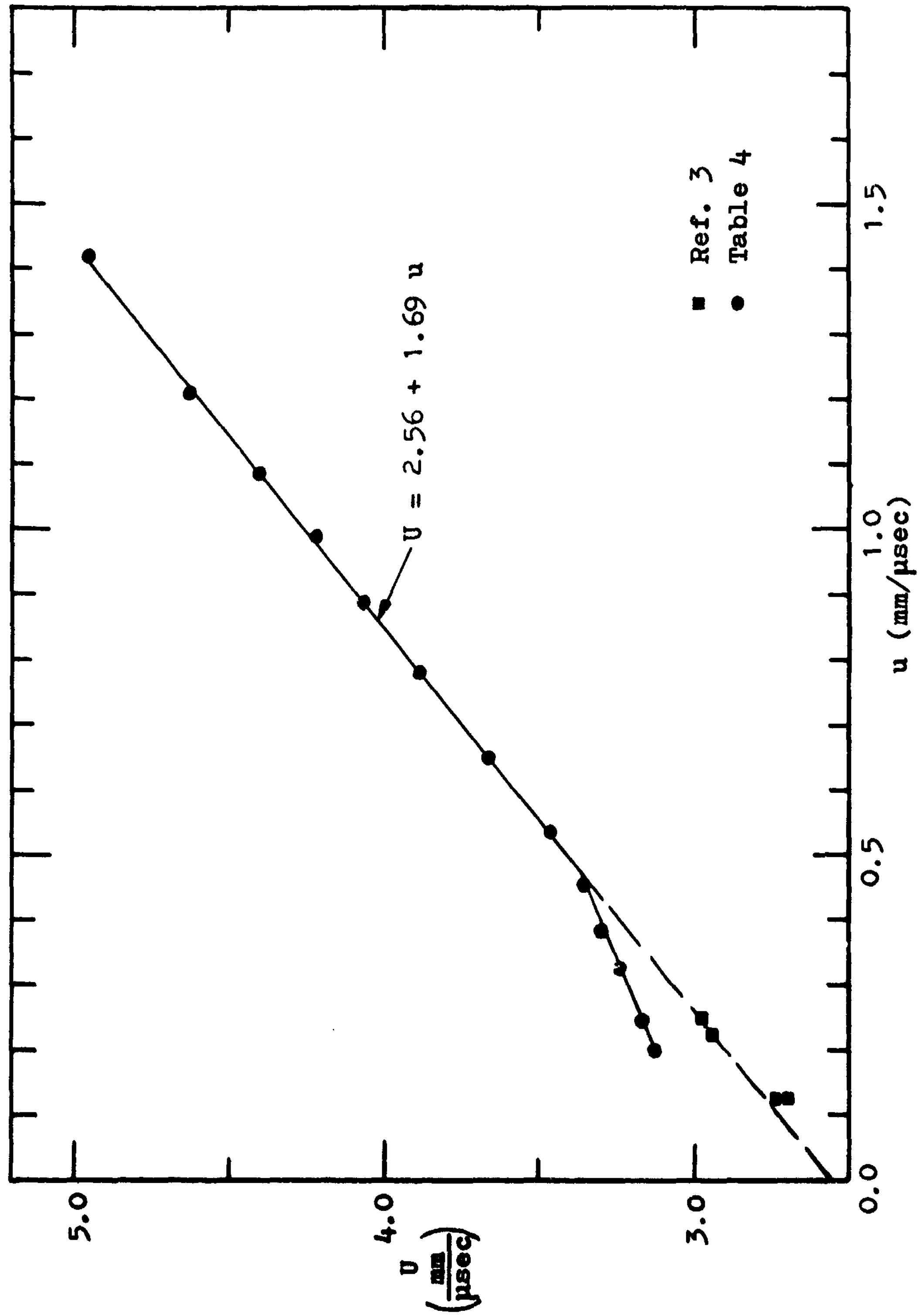

FIG. 7. SHOCK VELOCITY (U) AS A FUNCTION OF THE PARTICLE VELOCITY (u) FOR PMMA, AS DERIVED FROM FIGS. 5 AND 6.

Figure 8 compares the U-X curve obtained from the 70-mm smear-camera records in the latest experiments (Table B2, Appendix B) with those from the 35-mm camera (Table A4, Appendix A) in recent previous work. The two curves are nearly everywhere within the data ranges shown in Fig. 6 and their separation is well within the experimental precision estimated for reduction of the data from the 35-mm records. It follows that a common U-X calibration curve can be used for both the standardized and modified gap test. It is also strongly indicated that the tetryl pellets CH 5213 and 1878-96 are indistinguishable, and that the different detonators used have no effect on the shock developed in the tetryl loaded plastic. The coincidence within experimental error of the curves of Fig. 8 was indicated earlier by the equivalent u-X data of Table 2 for which all data were obtained with the 70-mm camera.

Inasmuch as the U-X curves are the same, the P-X curves for the standardized and modified gap tests must also be the same. Heretofore, except for the two indirect determinations of Reference 3, we have made no u-X measurements, and the calibration curves were derived from shock-velocity measurements only; in other words, the calibration curves were P_U vs X curves. In Fig. 9, the P-X curve (modified gap test) is compared with the most recent P_U' vs X curve (standard gap test); the prime denotes a set of constants slightly different from those of Eq. (1), (see Appendix A). Up to X = 40 mm, the two curves are experimentally the same. Beyond X = 40 mm, there is a divergence of P_U' from P, similar to that already described in the Table 4 data. It should be remarked that the lower pressures on the P vs X curve at X $\sim$ 100 mm are more in accord with the small damage observed in the shocked PMMA[9] than are the corresponding P_U' values. Shocked PMMA rods (initially 127 mm long) have been recovered by firing them into water. Much of the free end of the rod remains in its original shape although it exhibits multiple internal fractures. Fig. 10 is a photograph of a 127-mm long PMMA rod compared to the piece of a similar rod recovered after a shot.

To obtain a common calibration curve for the standard and modified gap tests, the U-X curves of Fig. 8 were averaged, and are shown in Table 5. The P-X and P_U'-X curves of Fig. 9 were averaged for the first 35 mm, after which the P-X data were used. This procedure results in a calibration curve in which the hump of Fig. 6 has been reduced; the curve is terminated at 100 mm to avoid the questionable trends at higher X (See Appendix A). In the future, U-X curves for the donor gap system will be obtained for each new lot of tetryl pellets. As long as they coincide with the present U-X calibration (Table 5), the present P-X curve can be used.

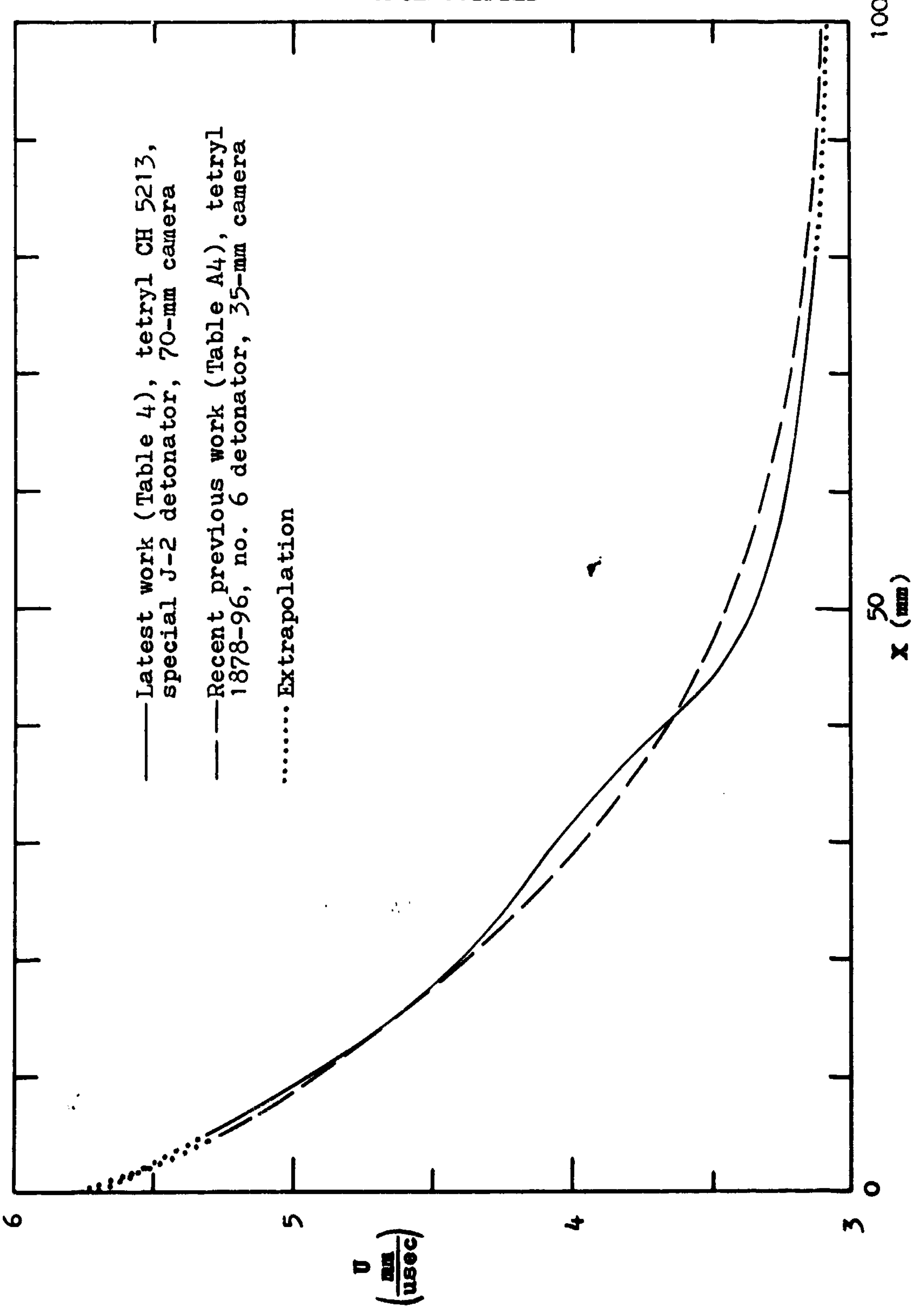

FIG. 8. COMPARISON OF U-X CALIBRATION CURVES.

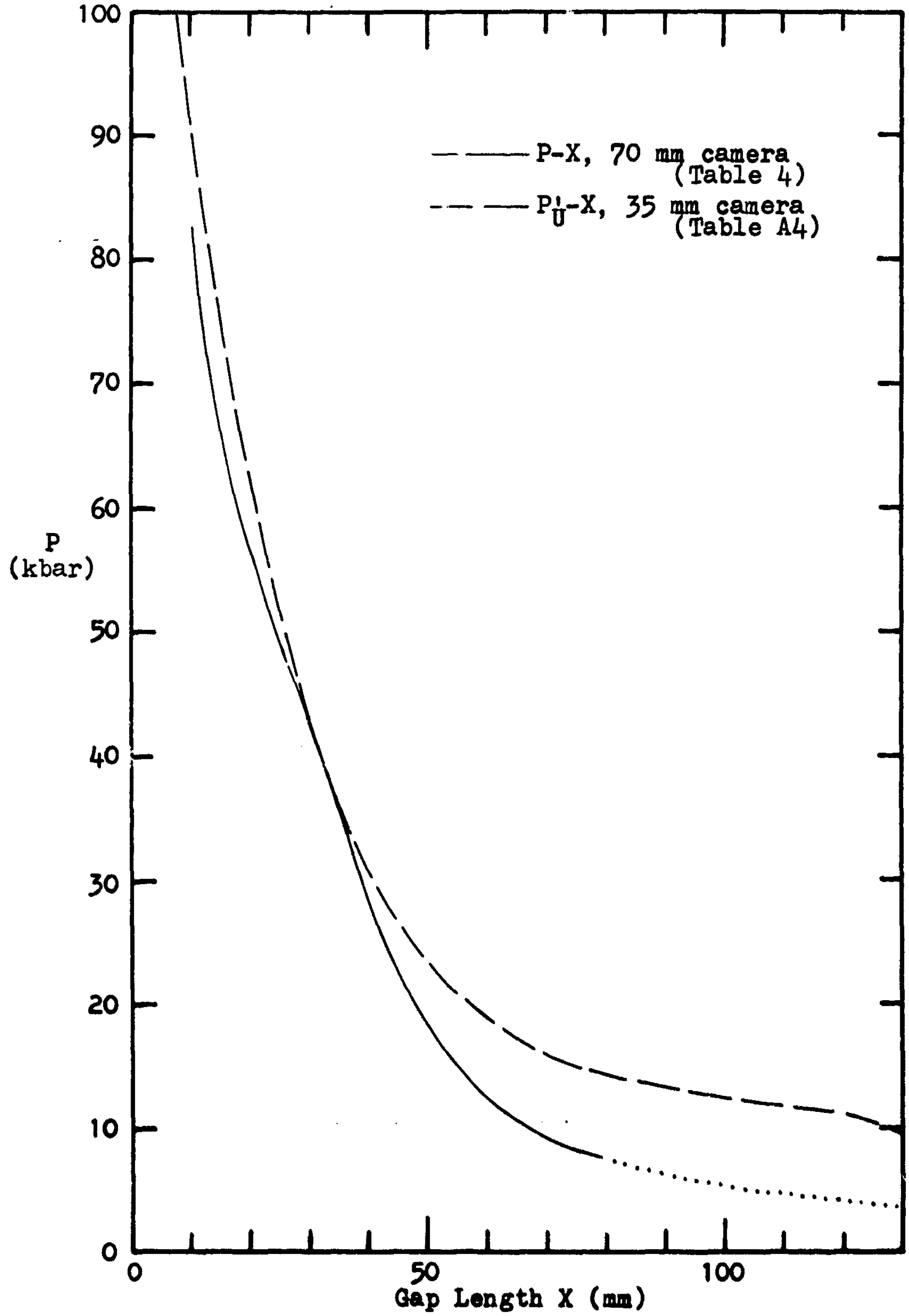

FIG. 9. COMPARISON OF P-X WITH P_U'-X CURVE.

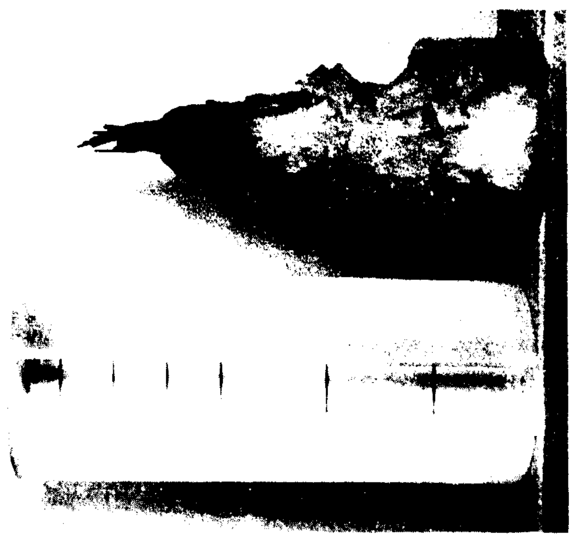

FIG. 10. PHOTOGRAPH OF A 127-mm LONG PMMA ROD COMPARED TO THE REMAINS OF A SIMILAR ROD RECOVERED AFTER A SHOT.

TABLE 5

CALIBRATION DATA FOR GAP TESTS

X (mm)	Shock Velocity U (mm/μsec)	Pressure P (kbar)
0	(5.75)	(126.0)
5	5.27	104.7
10	4.94	86.2
15	4.63	69.9
20	4.39	58.7
25	4.19	50.0
30	4.01	42.4
35	3.84	35.7
40	3.66	28.1
45	3.50	22.0
50	3.40	18.0
55	3.34	14.9
60	3.28	12.4
70	3.20	9.2
80	3.15	7.4
90	3.12	6.2
100	3.10	5.3

We believe that the calibration data (Table 5) present the best relationships (both U-X and P-X) that we can obtain with the current experimental techniques. It is hoped that in future work, the low-pressure end of the curve can be studied with quartz pressure gages.

This report has so far presented data from studies of the standard donor/gap system, and has shown that two lots of tetryl pellets (CH5213 and 1878-96) produced the same U vs X curve in the standard PMMA gap. While this report was being prepared, a new lot of tetryl pellets* were received and tested; they too produced a U vs X curve experimentally identical to those of Fig. 8. However, the earliest lot of tetryl pellets (1878-5), studied five years ago, produced a U-X curve appreciably different from those of Fig. 8. Consequently, the $P_U^{\dagger}$-X curve, reported in the open literature[3] for these pellets, differs from both the $P_U^{\dagger}$-X and P-X curves reported here.

Fig. 11 shows the present P-X calibration curve and the $P_U^{\dagger}$-X curve obtained with tetryl 1878-5 five years ago[3]. The difference in the two curves is large. It is impossible to say whether the difference arises from a difference in the tetryl pellets, or in the data collection and reduction, or in both. But it is quite evident that the old curve is inapplicable to the present donor/gap system except in the range of X = 45 to 65 mm (P = 22 to 10.5 kbar) where it fortuitously coincides with the present calibration curve.

SUMMARY AND CONCLUSIONS

1. Most solids exhibit a linear relationship between shock velocity and particle velocity. The present work shows that this relationship for PMMA in the standardized donor/gap system holds only down to a pressure of about 20 kbar.

2. The U-u relationship for PMMA of these dimensions has not been completely defined for pressures below 20 kbar.

3. It is, therefore, necessary to measure both shock and particle velocities as a function of gap thickness in making the low pressure calibrations.

4. A method of obtaining the initial free-surface velocity (u_{fs}) has been developed and is reported. Measurements of u_{fs} are used to obtain the necessary particle velocities.

---

*Tetryl 1878-125. Calibration data will be presented in a subsequent report.

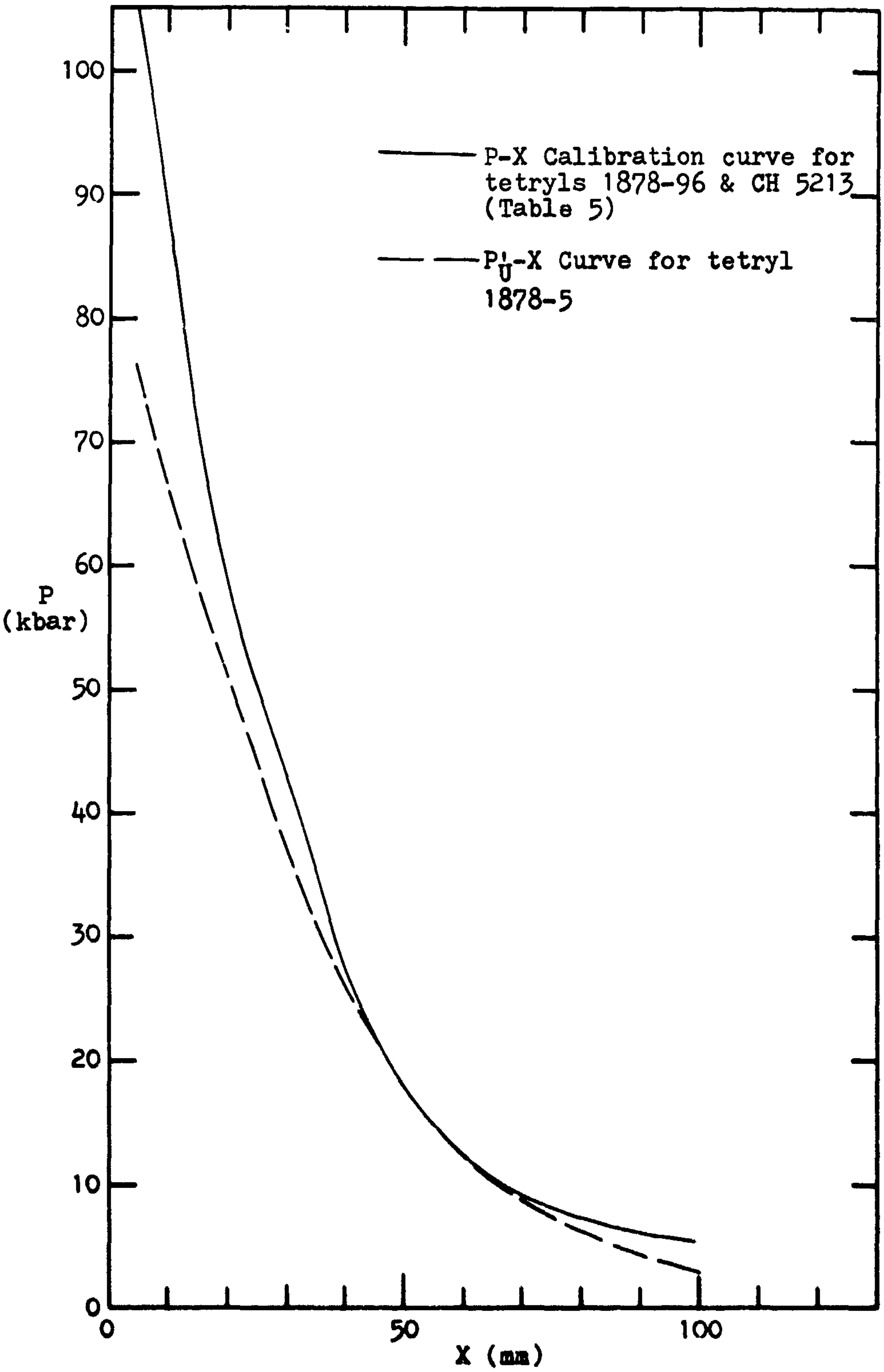

FIG. 11. COMPARISON OF PRESENT CALIBRATION WITH EARLIEST CALIBRATION.

5. From the current work, valid calibration curves for the tetryl/PMMA system of both the standardized and modified gap tests have been presented. The U vs X curves are essentially the same as those that have been used recently for the standardized gap test. The P vs X curves are the same $P \geq 20$ kbar, but differ in the low pressure region.

ACKNOWLEDGMENT

The authors wish to thank J. Schneider for his painstaking work in making the surface velocity and the shock velocity (70-mm camera) measurements, and A. R. Clairmont for his equally careful work with the 35-mm camera. We are also grateful for the assistance of G. E. Roberson and J. H. Oliphant in the firings, and of J. P. Toscano and I. Jaffe in interpreting the records.

REFERENCES

1. E. H. Eyster, L. C. Smith and S. R. Walton, "The Sensitivity of High Explosives to Pure Shocks", NOLM 10,336 (14 Jul 1949). Unclassified.

2. G. P. Cachia and E. G. Whitbread, "The Initiation of Explosives by Shock", Proc.Roy.Soc. 246A, 268-73 (1958).

3. I. Jaffe, R. Beauregard, and A. Amster, "Determination of the Shock Pressure Required to Initiate Detonation of an Acceptor in the Shock Sensitivity Test", ARS Jour. 32, 22-25 (1962). Also NAVORD Report 6876 (1960).

4. W. B. Garn, "Determination of Unreacted Hugoniot for Liquid TNT", J. Chem. Phys. 30, 819-22 (1959).

5. V. S. Ilyukin, P. F. Pokhil, O. K. Rozanov, and N. S. Shvedova, "Measurement of the Shock Adiabats of Cast Trinitrotoluene, Crystalline Hexogene and Nitromethane", Proc.Aca.Sci. USSR, 5, 337-340 (1960).

6. S. J. Jacobs, T. P. Liddiard, and B. E. Drimmer, "The Shock-to-Detonation Transition in Solid Explosives", 9th Symposium (International) on Combustion, 517-26, Academic Press, N.Y.C. (1963).

7. D. Price and I. Jaffe, "Large Scale Gap Test: Interpretation of Results for Propellants", ARS Jour.31, 595-99 (1961). Also NAVWEPS Report 7401 (1961).

8. T. P. Liddiard, Jr. and S. J. Jacobs, "The Initiation of Reactions in Explosives by Shocks", NOLTR 64-53, in preparation.

9. I. Jaffe, J. Toscano, and D. Price, "Behavior of Plexiglas Under Shock Loading by a Tetryl Donor", NOLTR 64-66 (2 Jul 1964).

10. N. L. Coleburn, "The Dynamic Compressibility of Solids from Single Experiments Using Light-Reflection Techniques", NAVWEPS Report 6026 (31 Oct 1960). Results for Plexiglas quoted in Ref. (6).

11. G. E. Duvall and G. R. Fowles, "Shock Waves", High Pressure Physics and Chemistry, Vol. 2, 209-291, Academic Press, N.Y.C. (1963).

12. J. M. Walsh and R. H. Christian, "Equation of State of Metals from Shock Wave Measurements", Phys.Rev. 97, 1544-56 (1955).

13. S. J. Jacobs, J. P. McLanahan,Jr., and E. C. Whitman, "A High Speed Focal Plane Shutter Framing Camera", Proc. 6th International Congress on High Speed Photography, The Hague, Sep 1962, T. Willink, Haarlem (1963) p.57; Jour.SMPTE, 72, 923 (1963).

14. T. P. Liddiard, Jr., B. E. Drimmer, and S. J. Jacobs, "Applications of the High-Speed Focal-Plane Shutter Camera to Explosives Research", ibid, p. 497 in Proceedings and p. 927 in Jour.SMPTE.

15. D. V. Keller and J. G. Trulio, "Mechanism of Spall in Lucite", J.Appl.Phys. 34, 172-5 (1963).

16. J. Toscano, I. Jaffe, and G. Roberson, "Large Scale Gap Test: Comparison of Tetryl and Pentolite Donors", AIAA Journal 1, 964-66 (1963). Also NOLTR 63-19.

Appendix A

CALIBRATION DATA OBTAINED WITH THE 35-mm SMEAR CAMERA

In the last few years, three calibrations of donor/PMMA systems similar to that of the standardized gap test (Fig. A1) have been made. In each case the smear-camera record of position (X) vs time (t) of the shock front in the PMMA provided the basic data.

The camera uses 35-mm film and has a writing speed of 1.3 mm/μsec. For a 100-mm long rod, we estimate that X can be read to 0.2 mm and t to 0.03 μsec. The first 3.2 mm of shock path are obscured by the shield between the donor and the rod; because of that and of optical disturbances, the earliest reading that can be taken is at about 5 mm and 1 μsec. Consequently, in the first (and steepest) portion of the X-t curve, reading errors of about 5% in each variable can be expected, whereas at the end of the curve (ca. 100 mm), errors will be of the order of magnitude of a few tenths of a per cent. It is, however, the U-X curve rather than the X-t curve that is required, and differentiation of the X-t curve to obtain the U-X curve can introduce errors in U greater than the sum of the errors in the corresponding values of X and t. As a result, we estimate that errors in any single determination of the velocity may range from 20% at 6 mm/μsec to less than 1% at 3 mm/μsec.

Some averaging and smoothing of the data can minimize errors and permit reproducible extrapolation into the 0 to 5 mm range where measurements cannot be made. In the earliest calibration[3], the X-t curve (average of 5 shots) was smoothed graphically, differentiated graphically, and the resultant U-X curve smoothed and extrapolated graphically. Subsequent work led to the present and preferred method of handling the data. It uses analytical procedures to smooth the graphically derived results.

Unfortunately, there is no quantitative guidance in the exact type of shock attenuation to expect nor any assurance that a single analytical expression can encompass the physical behavior over the entire range studied. On the contrary, previous results[9] suggest the possibility of change in the nature of shock decay at path lengths of about 25 mm, 70 mm, and 100 mm. Under these circumstances, graphical reduction of the data from X vs t to U=(dX/dt) vs X was carried out independently by two people. Each smoothed and averaged all X-t data; from the average curve, the U-X curve was obtained.

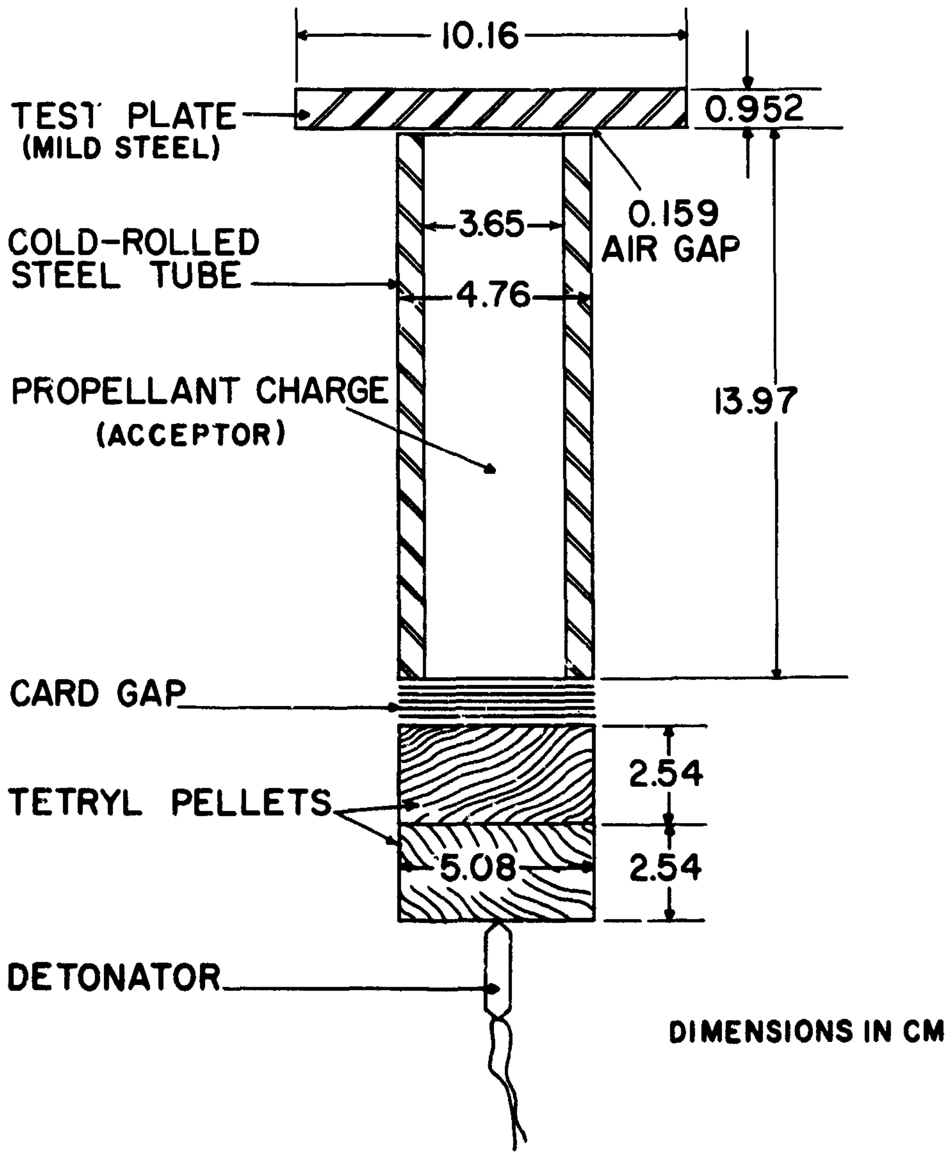

FIG. A1. CHARGE ASSEMBLY AND DIMENSIONS FOR NOL STANDARDIZED GAP TEST

The results were then compared with smoothed curves obtained by using the raw X vs t data in machine programs designed to fit the data to (1) an exponential function, and (2) various polynomials. It was found that the resulting U vs X curves from the analytical procedure most closely approximated the two graphically derived curves when the exponential

$$X(t) = at + c - ce^{-mt} \tag{A1}$$

was used; a, c, and m are constants. This is for the range of X = 0 to 60 or 70 mm and it is graphically joined to the appropriate polynomial, generally the 4th degree, for X = 60 or 70 mm and greater. At longer path lengths (85 mm and above), it was sometimes necessary to use the graphically smoothed curve because no polynomial approximated it adequately. This range is, of course, the region of greatest accuracy of the graphical method. This current procedure requires multiple comparisons and computations for each calibration. Chief dependence on the smoothed curve is for extrapolation and to obtain averaged values in which the errors are small. We believe that the error in U at X = 5 mm is about 5% if data for five shots are averaged and smoothed as described. Thus for tetryl at U = 5.3 mm/usec the value might be in error by about ± 0.13; this is somewhat larger than the range of data at X = 5 found with the 70-mm camera, as would be expected. With increasing path lengths, the error in U should decrease.

The present method of data reduction supersedes a less satisfactory procedure reported earlier[16]. Reasons for discarding the first analytical treatment are given in Appendix II of Ref. 9.

Tables A1 to A3 contain the X vs t data read from the smear-camera records for: (a) tetryl loading of a PMMA rod (cylinder with two machined flats), (b) tetryl loading of a PMMA block, and (c) pentolite loading of a PMMA rod. The smoothed data obtained with the current method of reduction appear in Table A4.

Comparison of the U-X data for the tetryl/cylinder and the tetryl/block systems show that the two curves are coincident X = 0 to 85 mm. Besides indicating that square and cylindrical cross-sections of the plastic are equivalent in attenuating the shock on the axis, the coincident curves also attest the reproducibility obtained with this method of data treatment. Results at X > 85 mm are not as satisfactory. Both the tetryl/block and pentolite/cylinder systems exhibit a more rapid drop in U with X than the tetryl/cylinder systems of Fig. 8. Further work would have to be done to determine if these irregularities are real.

TABLE A1

RAW DATA: TETRYL ON PMMA ROD WITH FLATS

Shot: A-144		A-166		A-167	A-175		A-176
Time (usec)	Distance (mm)	Time (usec)	Distance (mm)	Time (usec)	Time (usec)	Distance (mm)	Time (usec)
0.53	(3.18)	0.52	(3.18)	0.52	0.66	(3.12)	0.62
1.76	9.53	1.31	7.18	1.31	1.62	8.20	1.62
3.09	15.88	2.10	11.18	2.09	2.74	13.28	2.70
4.49	22.50	2.96	15.18	2.96	3.83	18.36	3.75
5.98	28.58	3.84	19.18	3.84	4.94	23.44	4.94
7.60	34.93	4.75	23.18	4.74	6.18	28.52	6.14
9.27	41.28	6.00	28.18	6.00	7.47	33.60	7.41
12.89	53.98	7.24	33.18	7.24	8.78	38.68	8.77
16.74	66.68	8.55	38.18	8.54	10.15	43.76	10.17
20.72	79.38	10.02	43.18	10.01	11.62	48.84	11.62
24.86	92.08	11.47	48.18	11.46	13.06	53.92	13.09
28.89	104.78	12.98	53.18	12.98	14.61	59.00	14.63
		15.98	63.18	15.98	16.10	64.08	16.18
		18.98	73.18	18.97	17.66	69.16	17.74
		22.14	83.18	22.14	19.25	74.24	19.33
		25.36	93.18	25.35	20.78	79.32	20.93
		28.56	103.18	28.55	22.44	84.40	22.54
		29.06	104.78	29.06	24.03	89.48	24.13
					25.63	94.56	25.70
					27.23	99.64	27.32
					28.90	104.72	29.01
					30.53	109.80	30.64
					32.21	114.88	32.30
					33.84	119.96	33.96
					35.52	125.04	35.67
					37.18	130.12	37.30

Tetryl 1878-96, 50.8-mm diam x 50.8-mm long, $\rho_0 = 1.51 \pm 0.01$ g/cc.
PMMA: flats 9 to 10-mm wide and about 50.6-mm apart on a rod of about 52-mm diam machined from flat stock 50.6-mm thick.

TABLE A2

RAW DATA: TETRYL ON PMMA BLOCK*

Expt. #1		Expt. #2		Expt. #3	
Time (μsec)	Distance (mm)	Time (μsec)	Distance (mm)	Time (μsec)	Distance (mm)
1.81	9.6	1.80	9.4	1.79	9.4
3.14	15.6	3.23	16.0	3.04	15.4
4.41	21.8	4.67	22.1	4.48	21.9
6.01	28.3	6.19	28.3	6.04	28.4
9.27	41.0	9.60	41.2	9.22	40.9
12.96	53.9	13.36	53.8	12.79	53.7
14.95	60.4	15.29	60.0	14.80	60.0
16.84	66.5	17.30	66.2	16.73	66.2
18.74	72.8	19.31	72.8	18.78	72.9
20.85	79.2	21.40	79.2	20.83	79.1
24.98	92.1	25.52	92.0	24.55	91.6
27.21	99.1	27.79	98.3	26.60	98.0
29.25	105.5	29.71	104.5	28.75	104.4

Tetryl 1878-96, 50.8-mm diam. x 50.8-mm long, $\rho_0 = 1.51 \pm 0.01$ g/cc.

PMMA 50.8-mm square x 101.6-mm long.

*Originally reported in Ref. (9).

TABLE A3

RAW DATA: PENTOLITE ON PMMA ROD WITH FLATS*

Expt. #1		Expt. #2		Expt. #3		Expt. #4	
Time (μsec)	Distance (mm)	Time (μsec)	Distance (mm)	Time (μsec)	Distance (mm)	Time (μsec)	Distance (mm)
1.21	7.2	1.87	10.4	1.31	8.0	1.18	7.2
3.83	20.0	3.76	18.9	2.89	16.0	2.01	11.5
5.69	28.0	5.82	28.1	5.85	28.9	4.08	21.2
7.71	35.7	7.70	35.3	7.75	35.9	7.64	36.0
10.26	44.5	10.36	45.0	10.19	44.3	10.19	45.5
12.68	52.4	12.84	53.6	13.14	53.1	13.88	58.0
15.73	62.0	16.07	64.2	17.69	68.5	18.07	71.3
23.40	85.7	20.74	79.0	19.99	75.5	21.63	82.8
25.53	92.2	23.84	89.0	22.23	82.3	24.53	92.0
27.43	97.7	26.96	98.6	25.78	93.6	27.34	100.5
28.87	102.2			28.86	102.8		

Pentolite 50/50 (PETN/TNT), ρ_o = 1.56 to 1.57 g/cc.

PMMA: flats about 47.6-mm apart on a rod of about 50.8-mm diam machined from 47.6-mm thick flat stock.

*Originally reported in Ref. (16).

TABLE A4

SMOOTHED CALIBRATION DATA

Donor/Gap	Tetryl/Cylinder		Tetryl/Block		Pent./Cylinder	
X (mm)	U (mm/μsec)	P'_U (kbar)	U (mm/μsec)	P'_U (kbar)	U (mm/μsec)	P'_U (kbar)
0	(5.59)	(131)	(5.56)	(129)	(6.21)	(175)
5	5.24	108	5.22	107	5.71	139
10	4.92	89.4	4.92	89.2	5.25	109
15	4.63	73.7	4.64	73.9	4.84	85.0
20	4.38	60.9	4.38	60.9	4.49	66.6
25	4.16	50.7	4.15	50.5	4.20	52.8
30	3.96	42.1	3.96	42.1	3.96	42.1
35	3.80	35.7	3.79	35.5	3.74	33.8
40	3.66		3.65		3.58	
45	3.54		3.52		3.44	
50	3.44		3.42		3.34	
55	3.38		3.34		3.26	
60	3.32		3.28		3.22	
65	3.26		3.22		3.22	
70	3.22		3.19		3.18	
75	3.18		3.18		3.14	
80	3.16		3.16		3.09	
85	3.14		3.10		3.04	
90	3.12		3.04		3.00	
95	3.11		3.00		2.94	
100	3.10		2.94		2.85	
105	3.09		2.88		2.74	
110	3.08					
115	3.06					
120	3.05					
125	3.02					
130	3.00					

In converting U-X data to pressure-distance data, the relations used are the hydrodynamic equation

$$P = \rho_0 \; U \; u \tag{A2}$$

and

$$U = 2.588 + 1.514 \; u, \tag{A3}$$

where the units are mm/usec. Eq. (A3) is one of the various Hugoniots reported for PMMA[3], and can be substituted in Eq. (A2) to give

$$P_U' = 10 \cdot 1.18 \; U \; (U - 2.588)/1.514, \tag{A4}$$

where the density is in g/cm^3 and the pressure is in kbar. The subscript U indicates that P_U' has been computed for measured values of this variable only; the prime indicates that the U-u relationship of Eq. (A3) has been used rather than the similar one fitting the data presented in the body of the report.

From Eqn's (A2) and (A3), it can easily be shown that

$$\frac{\Delta P}{P} = \frac{\Delta U}{U} + \frac{\Delta U}{U - 2.588} \quad . \tag{A5}$$

Consequently any error in U will be magnified by converting it to the corresponding pressure value. A 1% error in U will, by Eq. (A5), result in a 2.8 to 4% error in P as U varies from 6 to 3.8 mm/usec. We have already shown in the main text that the error of such conversion for $U < 3.8$ mm/usec becomes much greater because of the failure of relationships such as Eq. (A3). Therefore, when only U-X data are available, it is preferable to compare different sets of calibration data on the basis of shock velocities rather than to convert the data, e.g., by Eq. (A4). Values of P_U' are given in Table A4 only for $P > 30$ kbar where P_U' is a good approximation to P.

Fig. A2 shows U vs X curves obtained with three different lots of tetryl pellets ($\rho_0 = 1.51$ g/cc). The lower dashed curve is for tetryl 1878-5 and was graphically derived[8]. The solid curve is an average of the three curves which are coincident within experimental precision: tetryl 1878-96 loading of a rod and of a block (Table A4) and tetryl CH5213 loading of a rod (Table 4). It is evident that although lots 1878-96 and CH5213 are very similar, both differ significantly from 1878-5. It is necessary, therefore, to calibrate every lot of pellets before interpreting the results they produce in the standardized gap test.

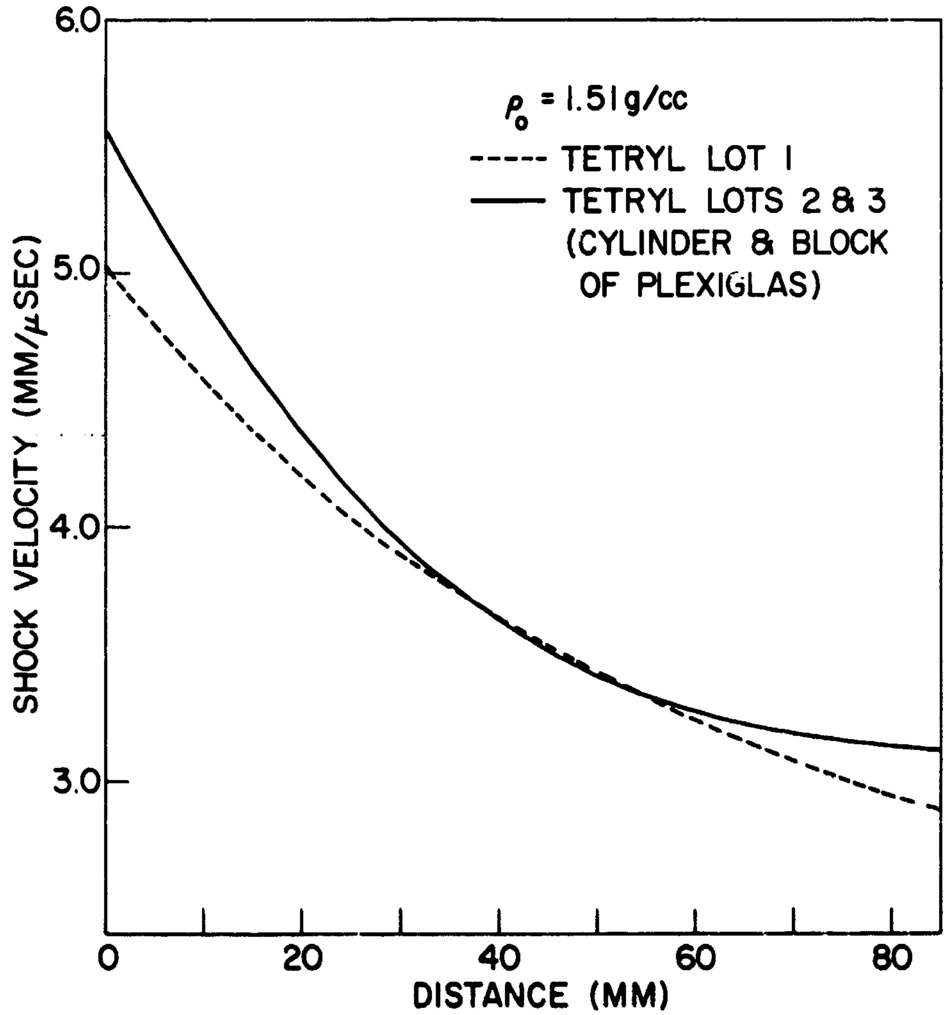

FIG. A2. SHOCK VELOCITY-DISTANCE CURVES FOR TETRYL LOADED PLEXIGLAS

In Fig. A3 the solid U vs X curve for the current tetryl pellets is compared with the U vs X curve produced by pentolite pellets (Table A4). For the first 30 mm of PMMA, the two curves obviously differ. Nevertheless, each of these donors gives the same initiating pressure for a given test acceptor. This has been shown by determining the 50% gap value, with each donor, of several acceptor explosives in the gap range of 4 - 53 mm, i.e., within the X range in which satisfactory U vs X curves are obtained by the present reduction procedure.

It was erroneously reported[16] earlier that pentolite and tetryl donors gave different initiation pressures for the same explosive. This is not true and appeared so only because the calibration curve for tetryl pellets 1878-5 was applied to tetryl pellets 1878-96. As has been shown, the two curves are very different.

Table A5 contains a corrected comparison of these two donors used to gap test three different explosives. It can be seen that each donor produced the same shock velocity at the end of the 50% gap to a precision of ± 2.5% of the mean, or better. The corresponding pressures will also be the same, but here the spread will be greater. Probably ± 10% in pressure is the best that can be expected even in the range $P_U' > 30$, where $P_U' = P$.

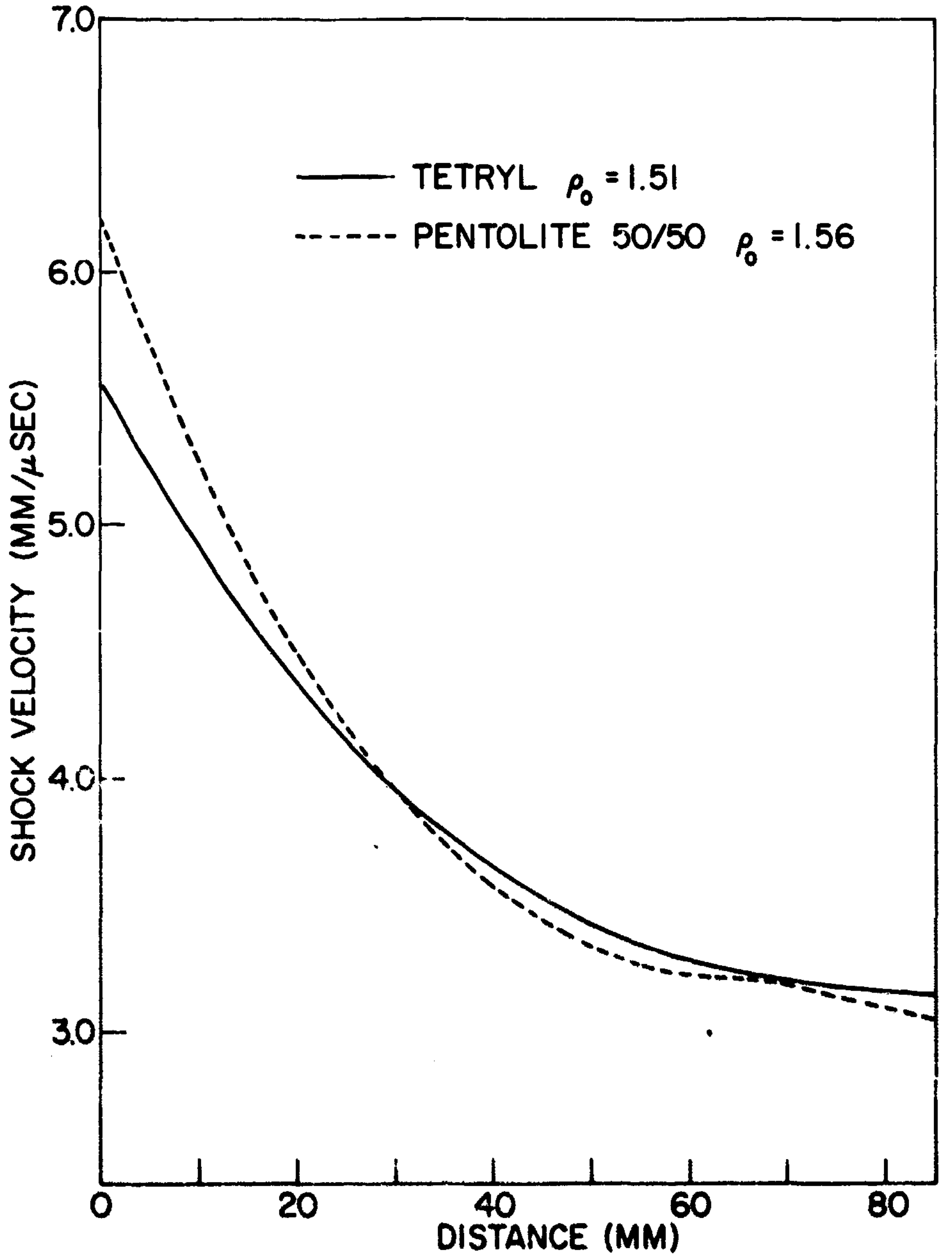

FIG. A3. SHOCK VELOCITY-DISTANCE CURVES FOR EXPLOSIVELY LOADED PLEXIGLAS

TABLE A5

GAP TEST RESULTS OBTAINED WITH TWO DIFFERENT DONORS

Material	50% Values				P'_U (kbar)	$\Delta P'_U$ (%)
	Donor*	Gap (mm)	Shock Velocity, U (mm/usec)	ΔU (%)		
NQ/Wax, 95/5	T	4.06	5.310		112.7	
1.55 g/cc	P	6.35	5.580		132.0	
			5.445	±2.5	122.3	± 8
NQ	T	11.7	4.815		83.7	
1.59 g/cc	P	13.5	4.955		92.5	
			4.885	±1.4		± 5
Comp B-3	T	53.1	3.400		**	
Cast	P	53.1	3.290			
			3.345	±1.7		

* T: Tetryl pellets Nb 1878-96, 1.51 g/cc.
P: Pentolite 50-50 pellets, 1.56 g/cc.

** Pressure of 16 kbar on current calibration curve, Table 5.

APPENDIX B

DETERMINING U AS A FUNCTION OF X FROM THE 70-MM, SMEAR-CAMERA RECORDS

In the case of the 70-mm records, the X - t curve for each smear-camera record was differentiated separately. The resulting U - X data were then averaged. This is in contrast to the procedure of Appendix A for the 35-mm camera data, where the averaging of all X - t data was done before differentiating.

Various methods of differentiating the X - t data can be used; to check these methods against one another record No. 144A was read in three different ways:

(1) The X - t Plot Method - The X - t data are obtained from the record with a comparator, plotted, and slopes taken from the resulting curve;

(2) The X - t Projection Method - An enlarged image of the record is projected on paper, a continuous pencil trace of the X - t curve is obtained, and slopes are taken directly from this curve; and

(3) The Direct Slope Method - Angles, which are converted to slopes, are read directly from the record with the comparator at fixed values of X.

Method (1) is straightforward and is the usual way of obtaining U - X data from smear-camera records. In Method (2) the shock-front curve on the smear-camera record is traced over with a hard, sharp pencil. The best possible fit to the trace is made using French curves as guides. If the process is carried out carefully, there will be no overlap in fitting curve segments together. This method has an advantage in being much more rapid than the other two. Method (3) requires the placement in the film plane of a grid with parallel lines, which cut through the shock-front trace, permitting identification of the position (X or t) at which a slope measurement is made.

The smoothed U - X results of the three methods, used in reading Record No. 144A, are in Table B1. The unsmoothed data, obtained by two readers from Record No. 144A, using the X - t plot method (Method (1)) are shown in Fig. B1. One reader's results show a small but definite hump in the curve, while the other reader's shows only a hint of such a hump. The slopes were taken from curves drawn from the same X - t data. In the comparison with the results of the other two methods, Table B1, the smoothed U - X data were picked off the curve of Fig. B1, this being fitted by eye to the two sets of unsmoothed U - X

TABLE B1

SMOOTHED U - X RESULTS USING THREE METHODS OF READING RECORD NO. 144A

X (mm)	U (mm/μsec)			
	Method # 1*	Method # 2	Method # 3	Mean
0	5.60	5.75	5.50	5.62
5	5.27	5.41	5.17	5.28
10	4.97	5.08	4.86	4.97
15	4.68	4.72	4.58	4.66
20	4.41	4.44	4.35	4.40
25	4.19	4.21	4.19	4.20
30	4.02	4.08	4.04	4.05
35	3.84	3.91	3.84	3.86
40	3.66	3.70	3.61	3.66
45	3.50	3.48	3.44	3.47
50	3.37	3.38	3.33	3.36
55	3.30	3.30	3.26	3.29
60	3.26	3.23	3.21	3.23
65	3.24	3.17	3.16	3.19
70	3.21	3.12	3.13	3.15
75	3.18	3.10	3.13	3.14
80	3.15	3.09	3.13	3.12

*Average of slopes obtained by two people from the same X - t data.

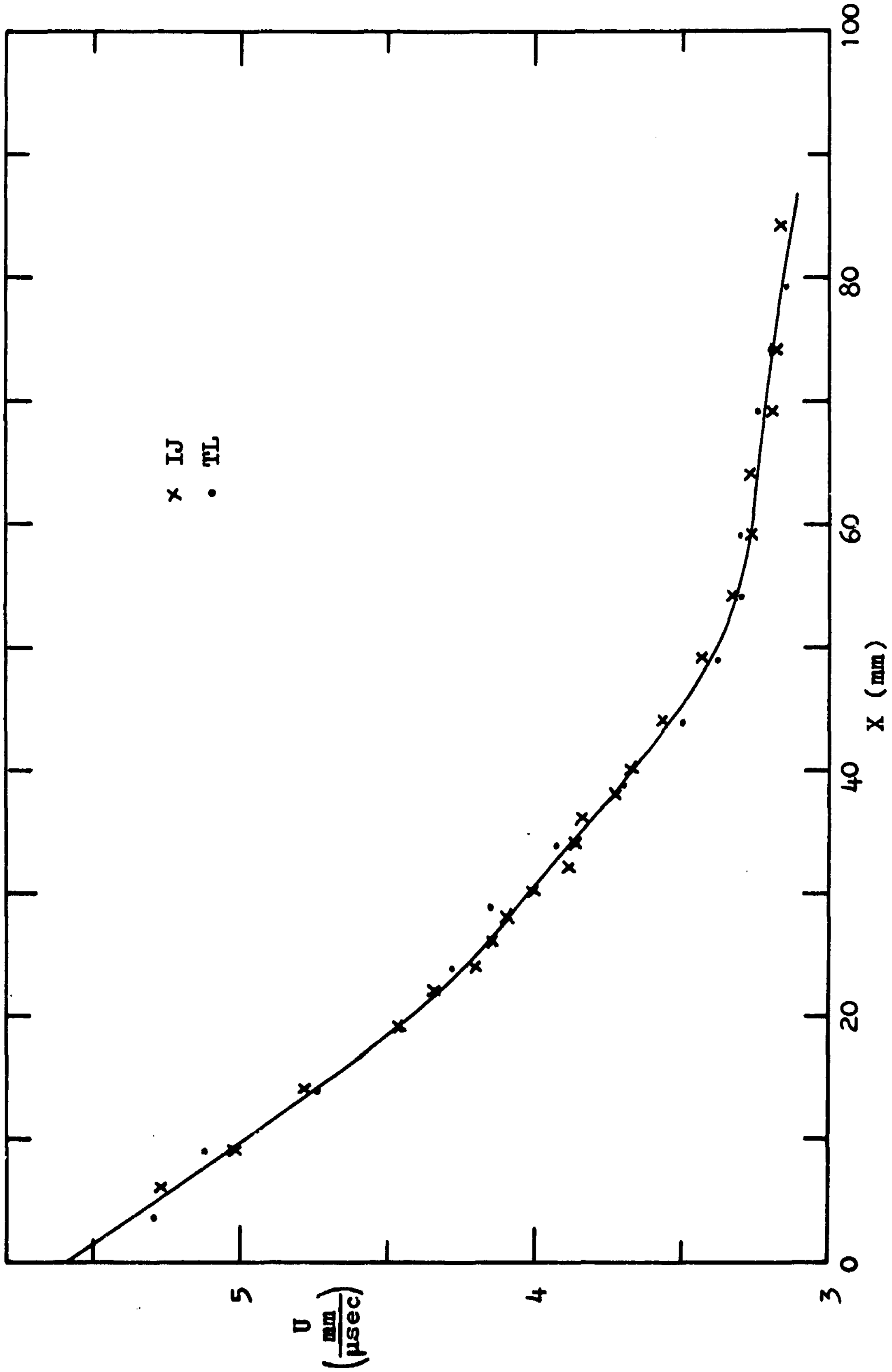

FIG. B1. U-X DATA OBTAINED FROM X-t PLOT OF RECORD NO. 144A BY TWO OBSERVERS, IJ & TL.

data. In Fig. B2 are the unsmoothed data obtained from the same record (144A) by the X - t projection method (Method #2) and the direct slope method (Method #3). One reader obtained both of these sets of data. All three sets of data fall close to each other, except below X = 20 mm, where the greatest deviation would be expected. Again, there is a small but clear hump in the curve. (See Fig. 6 of main text.) Record No. 144D was read by Methods (2) and (3); it gave curves falling within ± 0.05 mm/usec of each other out to X = 40 mm, the limit of readability. Since X - t projection (Method 2) is the easiest of the three methods to use and apparently is capable of as precise measurement as the others, it was used to obtain the U - X data from the remaining records.

The results from seven records are given in Table B2. The "Mean" column contains U values obtained from seven records to X = 40 mm; from six records to X = 50 mm; from five records to X = 65 mm; from four records to X = 70 mm; and from two records out to X = 80 mm. Ordinarily, there is danger in using the mean values obtained from varying the numbers in a sample. The smaller the number used in a sample, the greater the possibility of introducing spurious displacements in the U - X curve at points where the number of data in the sample is changed. However, in this particular case, when five values of U are used from X = 0 to X = 65 mm, using Method (2), the resulting values do not change by more than 0.5% from those obtained with the corresponding possible combinations of seven, or of six, of the values given in Table B2. Beyond X = 65 mm, it apparently makes little difference how many values are used in obtaining the mean since the reading errors are quite small at this end of the X - t curve, as described in Appendix A.

TABLE B2

SMOOTHED U - X DATA FOR SEVEN 70-MM
SMEAR-CAMERA RECORDS

X (mm)	U (mm/μsec)							
	A*	B	D**	H	I	J	K	Mean
0	5.62		5.68					
5	5.28	5.21	5.39	5.33	5.32	5.38	5.20	5.30
10	4.97	4.88	4.97	5.01	4.94	4.99	4.90	4.95
15	4.66	4.54	4.65	4.67	4.60	4.66	4.59	4.62
20	4.40	4.34	4.40	4.45	4.38	4.44	4.36	4.40
25	4.20	4.15	4.21	4.28	4.20	4.23	4.21	4.21
30	4.05	4.02	4.08	4.12	4.08	4.08	4.02	4.06
35	3.86	3.85	3.94	3.97	3.90	3.84	3.78	3.88
40	3.66	3.64	3.74	3.66	3.69	3.60	3.61	3.66
45	3.47	3.45	—	3.42	3.49	3.50	3.43	3.46
50	3.36	3.37	—	3.34	3.31	3.41	3.31	3.35
55	3.29	3.29	—	3.32	—	3.31	3.29	3.30
60	3.23	3.25	—	3.22	—	3.27	3.23	3.24
65	3.19	3.21	—	3.21	—	3.25	3.20	3.21
70	3.15	—	—	3.14	—	3.21	3.18	3.17
75	3.14	—	—	—	—	3.15	—	3.15
80	3.12	—	—	—	—	3.13	—	3.13

* Average values using Methods (1), (2), and (3).
** Average values using Methods (2) and (3).
All others by Method (2) only.

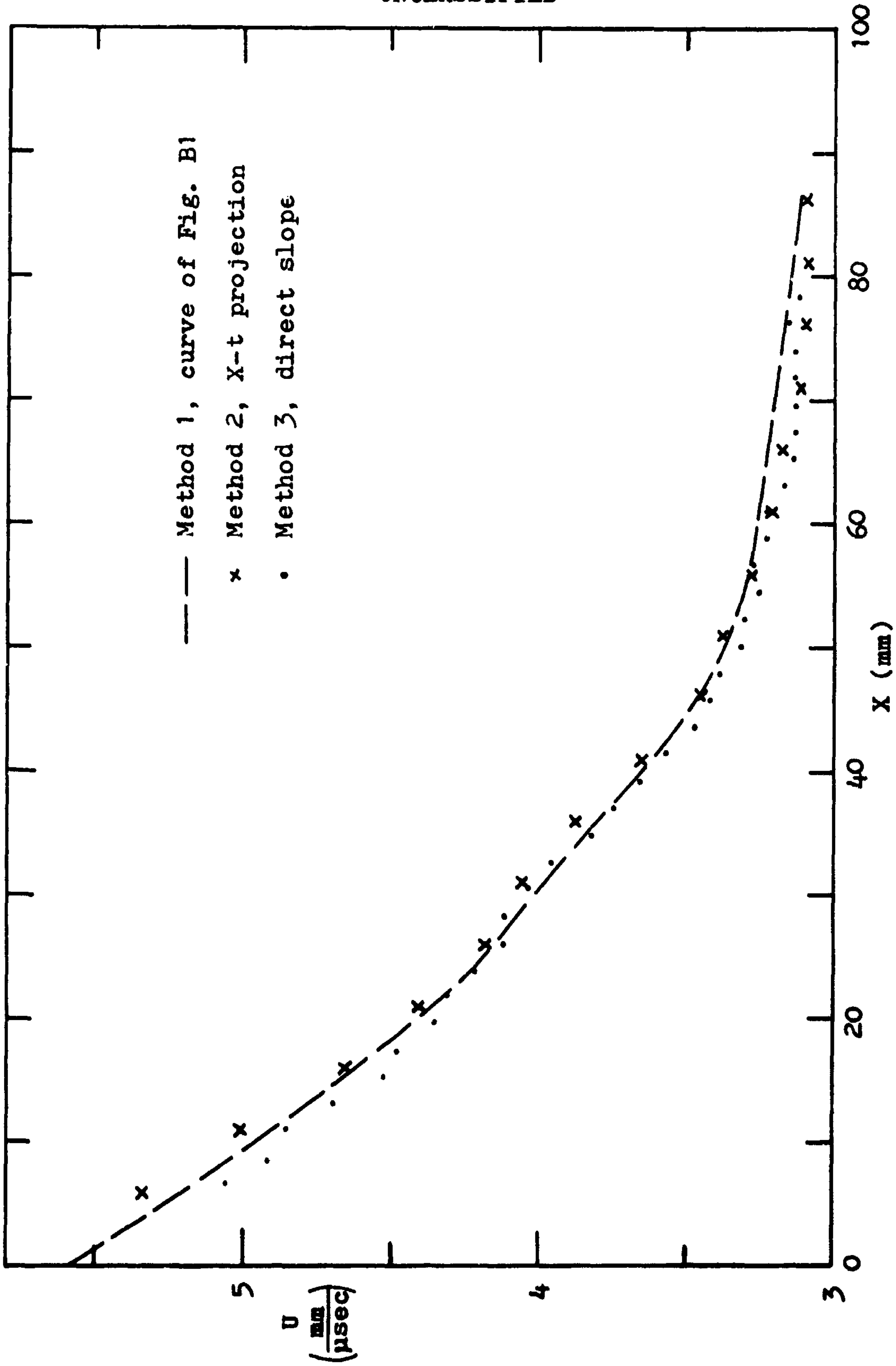

FIG. B2. U-X DATA ON RECORD NO. 144A OBTAINED BY THE X-t PROJECTION AND DIRECT SLOPE METHODS.

UNCLASSIFIED

Security Classification

DOCUMENT CONTROL DATA - R&D

(Security classification of title, body of abstract and indexing annotation must be entered when the overall report is classified)

1. ORIGINATING ACTIVITY (Corporate author) U. S. Naval Ordnance Laboratory White Oak, Silver Spring, Md.	2a. REPORT SECURITY CLASSIFICATION Unclassified 2b. GROUP --

3. REPORT TITLE

Recalibration of Standard Card-Gap Test

4. DESCRIPTIVE NOTES (Type of report and inclusive dates)

--

5. AUTHOR(S) (Last name, first name, initial)

Liddiard, Thomas P., Jr.
Price, Donna

6. REPORT DATE	7a. TOTAL NO. OF PAGES	7b. NO. OF REFS
20 Aug 65	46	16

8a. CONTRACT OR GRANT NO.	9a. ORIGINATOR'S REPORT NUMBER(S)
b. PROJECT NO.	NOLTR 65-43
c. WepTasks:RMMO-51042/212-1/F009-0802 and RMMP-22149/ d. 212/F009-06-11	9b. OTHER REPORT NO(S) (Any other numbers that may be assigned this report) --

10. AVAILABILITY/LIMITATION NOTICES

Qualified Requestors may obtain from DDC.

11. SUPPLEMENTARY NOTES	12. SPONSORING MILITARY ACTIVITY
--	Bureau of Naval Weapons

13. ABSTRACT

A new calibration of peak pressure (P) vs gap length (X) is presented for the NOL standardized and modified gap tests. It is shown that experimental values of both shock velocity (U) and particle velocity (u) are required to obtain a valid P-X curve at low pressures, because the normally linear U-u curve for the gap material exhibits a discontinuity at about X = 50 mm. The initial free-surface velocity ($u_{fs} \cong 2U$) is determined by monitoring films placed at the end of the gap.

DD FORM 1 JAN 64 1473

UNCLASSIFIED

Security Classification

UNCLASSIFIED

Security Classification

14. KEY WORDS	LINK A		LINK B		LINK C	
	ROLE	WT	ROLE	WT	ROLE	WT
GAP TEST						
EXPLOSIVES						
SENSITIVITY						
CALIBRATION						
PLEXIGLAS						
SHOCK VELOCITY						
PARTICLE VELOCITY						
FOIL TECHNIQUE						

INSTRUCTIONS

1. ORIGINATING ACTIVITY: Enter the name and address of the contractor, subcontractor, grantee, Department of Defense activity or other organization *(corporate author)* issuing the report.

2a. REPORT SECURITY CLASSIFICATION: Enter the overall security classification of the report. Indicate whether "Restricted Data" is included. Marking is to be in accordance with appropriate security regulations.

2b. GROUP: Automatic downgrading is specified in DoD Directive 5200.10 and Armed Forces Industrial Manual. Enter the group number. Also, when applicable, show that optional markings have been used for Group 3 and Group 4 as authorized.

3. REPORT TITLE: Enter the complete report title in all capital letters. Titles in all cases should be unclassified. If a meaningful title cannot be selected without classification, show title classification in all capitals in parenthesis immediately following the title.

4. DESCRIPTIVE NOTES: If appropriate, enter the type of report, e.g., interim, progress, summary, annual, or final. Give the inclusive dates when a specific reporting period is covered.

5. AUTHOR(S): Enter the name(s) of author(s) as shown on or in the report. Enter last name, first name, middle initial. If military, show rank and branch of service. The name of the principal author is an absolute minimum requirement.

6. REPORT DATE: Enter the date of the report as day, month, year; or month, year. If more than one date appears on the report, use date of publication.

7a. TOTAL NUMBER OF PAGES: The total page count should follow normal pagination procedures, i.e., enter the number of pages containing information.

7b. NUMBER OF REFERENCES: Enter the total number of references cited in the report.

8a. CONTRACT OR GRANT NUMBER: If appropriate, enter the applicable number of the contract or grant under which the report was written.

8b, 8c, & 8d. PROJECT NUMBER: Enter the appropriate military department identification, such as project number, subproject number, system numbers, task number, etc.

9a. ORIGINATOR'S REPORT NUMBER(S): Enter the official report number by which the document will be identified and controlled by the originating activity. This number must be unique to this report.

9b. OTHER REPORT NUMBER(S): If the report has been assigned any other report numbers *(either by the originator or by the sponsor)*, also enter this number(s).

10. AVAILABILITY/LIMITATION NOTICES: Enter any limitations on further dissemination of the report, other than those imposed by security classification, using standard statements such as:

(1) "Qualified requesters may obtain copies of this report from DDC."

(2) "Foreign announcement and dissemination of this report by DDC is not authorized."

(3) "U. S. Government agencies may obtain copies of this report directly from DDC. Other qualified DDC users shall request through ________________."

(4) "U. S. military agencies may obtain copies of this report directly from DDC. Other qualified users shall request through ________________."

(5) "All distribution of this report is controlled. Qualified DDC users shall request through ________________."

If the report has been furnished to the Office of Technical Services, Department of Commerce, for sale to the public, indicate this fact and enter the price, if known.

11. SUPPLEMENTARY NOTES: Use for additional explanatory notes.

12. SPONSORING MILITARY ACTIVITY: Enter the name of the departmental project office or laboratory sponsoring *(paying for)* the research and development. Include address.

13. ABSTRACT: Enter an abstract giving a brief and factual summary of the document indicative of the report, even though it may also appear elsewhere in the body of the technical report. If additional space is required, a continuation sheet shall be attached.

It is highly desirable that the abstract of classified reports be unclassified. Each paragraph of the abstract shall end with an indication of the military security classification of the information in the paragraph, represented as *(TS)*, *(S)*, *(C)*, or *(U)*.

There is no limitation on the length of the abstract. However, the suggested length is from 150 to 225 words.

14. KEY WORDS: Key words are technically meaningful terms or short phrases that characterize a report and may be used as index entries for cataloging the report. Key words must be selected so that no security classification is required. Identifiers, such as equipment model designation, trade name, military project code name, geographic location, may be used as key words but will be followed by an indication of technical context. The assignment of links, rules, and weights is optional.

UNCLASSIFIED

Security Classification

Naval Ordnance Laboratory, White Oak, Md.
(NOL technical report 65-43)
RECALIBRATION OF STANDARD CARD-GAP TEST, by T. P. Liddiard, jr and Donna Price. 20 Aug. 1965. v.p. charts, tables diagrs. BuWeps tasks RMMP-22149/212/F009-06-11 and RMMO-51042 212-1/F009-08-02.

UNCLASSIFIED

A new calibration of peak pressure (P) vs gap length (X) is presented for the NOL standardized and modified gap tests. It is shown that experimental values of both shock velocity (U) and particle velocity (u) are required to obtain a valid P-X curve at low pressures, because the normally linear U-u curve for the gap material exhibits a discontinuity at about X = 50 mm. The initial free-surface velocity (u_{fs} = 20) is determined by monitoring films placed at the end of the gap.

1. Explosives - Gap tests
2. Explosives - Sensitivity
I. Title
II. Liddiard, Thomas P., jr.
III. Price, Donna, jt. author
IV. Project
V. Project

Abstract card is unclassified.

Naval Ordnance Laboratory, White Oak, Md.
(NOL technical report 65-43)
RECALIBRATION OF STANDARD CARD-GAP TEST, by T. P. Liddiard, jr and Donna Price. 20 Aug. 1965. v.p. charts, tables diagrs. BuWeps tasks RMMP-22149/212/F009-06-11 and RMMO-51042 212-1/F009-08-02.

UNCLASSIFIED

A new calibration of peak pressure (P) vs gap length (X) is presented for the NOL standardized and modified gap tests. It is shown that experimental values of both shock velocity (U) and particle velocity (u) are required to obtain a valid P-X curve at low pressures, because the normally linear U-u curve for the gap material exhibits a discontinuity at about X = 50 mm. The initial free-surface velocity (u_{fs} = 20) is determined by monitoring films placed at the end of the gap.

1. Explosives - Gap tests
2. Explosives - Sensitivity
I. Title
II. Liddiard, Thomas P., jr.
III. Price, Donna, jt. author
IV. Project
V. Project

Abstract card is unclassified.

Naval Ordnance Laboratory, White Oak, Md.
(NOL technical report 65-43)
RECALIBRATION OF STANDARD CARD-GAP TEST, by T. P. Liddiard, jr and Donna Price. 20 Aug. 1965. v.p. charts, tables diagrs. BuWeps tasks RMMP-22149/212/F009-06-11 and RMMO-51042 212-1/F009-08-02.

UNCLASSIFIED

A new calibration of peak pressure (P) vs gap length (X) is presented for the NOL standardized and modified gap tests. It is shown that experimental values of both shock velocity (U) and particle velocity (u) are required to obtain a valid P-X curve at low pressures, because the normally linear U-u curve for the gap material exhibits a discontinuity at about X = 50 mm. The initial free-surface velocity (u_{fs} = 20) is determined by monitoring films placed at the end of the gap.

1. Explosives - Gap tests
2. Explosives - Sensitivity
I. Title
II. Liddiard, Thomas P., jr.
III. Price, Donna, jt. author
IV. Project
V. Project

Abstract card is unclassified.

Naval Ordnance Laboratory, White Oak, Md.
(NOL technical report 65-43)
RECALIBRATION OF STANDARD CARD-GAP TEST, by T. P. Liddiard, jr and Donna Price. 20 Aug. 1965. v.p. charts, tables diagrs. BuWeps tasks RMMP-22149/212/F009-06-11 and RMMO-51042 212-1/F009-08-02.

UNCLASSIFIED

A new calibration of peak pressure (P) vs gap length (X) is presented for the NOL standardized and modified gap tests. It is shown that experimental values of both shock velocity (U) and particle velocity (u) are required to obtain a valid P-X curve at low pressures, because the normally linear U-u curve for the gap material exhibits a discontinuity at about X = 50 mm. The initial free-surface velocity (u_{fs} = 20) is determined by monitoring films placed at the end of the gap.

1. Explosives - Gap tests
2. Explosives - Sensitivity
I. Title
II. Liddiard, Thomas P., jr.
III. Price, Donna, jt. author
IV. Project
V. Project

Abstract card is unclassified.

Naval Ordnance Laboratory, White Oak, Md.
(NOL technical report 65-43)
RECALIBRATION OF STANDARD CARD-GAP TEST, by T. P. Liddiard, jr and Donna Price. 20 Aug. 1965. v.p. charts, tables diagrs. BuWeps tasks RMMP-22149/212/F009-06-11 and RMMO-51042 212-1/F009-08-02.

UNCLASSIFIED

A new calibration of peak pressure (P) vs gap length (X) is presented for the NOL standardized and modified gap tests. It is shown that experimental values of both shock velocity (U) and particle velocity (u) are required to obtain a valid P-X curve at low pressures, because the normally linear U-u curve for the gap material exhibits a discontinuity at about X = 50 mm. The initial free-surface velocity (u_{fs} = 2U) is determined by monitoring films placed at the end of the gap.

1. Explosives - Gap tests
2. Explosives - Sensitivity

I. Title
II. Liddiard, Thomas P., jr.
III. Price, Donna, jt. author
IV. Project
V. Project

Abstract card is unclassified.

Naval Ordnance Laboratory, White Oak, Md.
(NOL technical report 65-43)
RECALIBRATION OF STANDARD CARD-GAP TEST, by T. P. Liddiard, jr and Donna Price. 20 Aug. 1965. v.p. charts, tables diagrs. BuWeps tasks RMMP-22149/212/F009-06-11 and RMMO-51042 212-1/F009-08-02.

UNCLASSIFIED

A new calibration of peak pressure (P) vs gap length (X) is presented for the NOL standardized and modified gap tests. It is shown that experimental values of both shock velocity (U) and particle velocity (u) are required to obtain a valid P-X curve at low pressures, because the normally linear U-u curve for the gap material exhibits a discontinuity at about X = 50 mm. The initial free-surface velocity (u_{fs} = 2U) is determined by monitoring films placed at the end of the gap.

1. Explosives - Gap tests
2. Explosives - Sensitivity

I. Title
II. Liddiard, Thomas P., jr.
III. Price, Donna, jt. author
IV. Project
V. Project

Abstract card is unclassified.

Naval Ordnance Laboratory, White Oak, Md.
(NOL technical report 65-43)
RECALIBRATION OF STANDARD CARD-GAP TEST, by T. P. Liddiard, jr and Donna Price. 20 Aug. 1965. v.p. charts, tables diagrs. BuWeps tasks RMMP-22149/212/F009-06-11 and RMMO-51042 212-1/F009-08-02.

UNCLASSIFIED

A new calibration of peak pressure (P) vs gap length (X) is presented for the NOL standardized and modified gap tests. It is shown that experimental values of both shock velocity (U) and particle velocity (u) are required to obtain a valid P-X curve at low pressures, because the normally linear U-u curve for the gap material exhibits a discontinuity at about X = 50 mm. The initial free-surface velocity (u_{fs} = 2U) is determined by monitoring films placed at the end of the gap.

1. Explosives - Gap tests
2. Explosives - Sensitivity

I. Title
II. Liddiard, Thomas P., jr.
III. Price, Donna, jt. author
IV. Project
V. Project

Abstract card is unclassified.

Naval Ordnance Laboratory, White Oak, Md.
(NOL technical report 65-43)
RECALIBRATION OF STANDARD CARD-GAP TEST, by T. P. Liddiard, jr and Donna Price. 20 Aug. 1965. v.p. charts, tables diagrs. BuWeps tasks RMMP-22149/212/F009-06-11 and RMMO-51042 212-1/F009-08-02.

UNCLASSIFIED

A new calibration of peak pressure (P) vs gap length (X) is presented for the NOL standardized and modified gap tests. It is shown that experimental values of both shock velocity (U) and particle velocity (u) are required to obtain a valid P-X curve at low pressures, because the normally linear U-u curve for the gap material exhibits a discontinuity at about X = 50 mm. The initial free-surface velocity (u_{fs} = 2U) is determined by monitoring films placed at the end of the gap.

1. Explosives - Gap tests
2. Explosives - Sensitivity

I. Title
II. Liddiard, Thomas P., jr.
III. Price, Donna, jt. author
IV. Project
V. Project

Abstract card is unclassified.